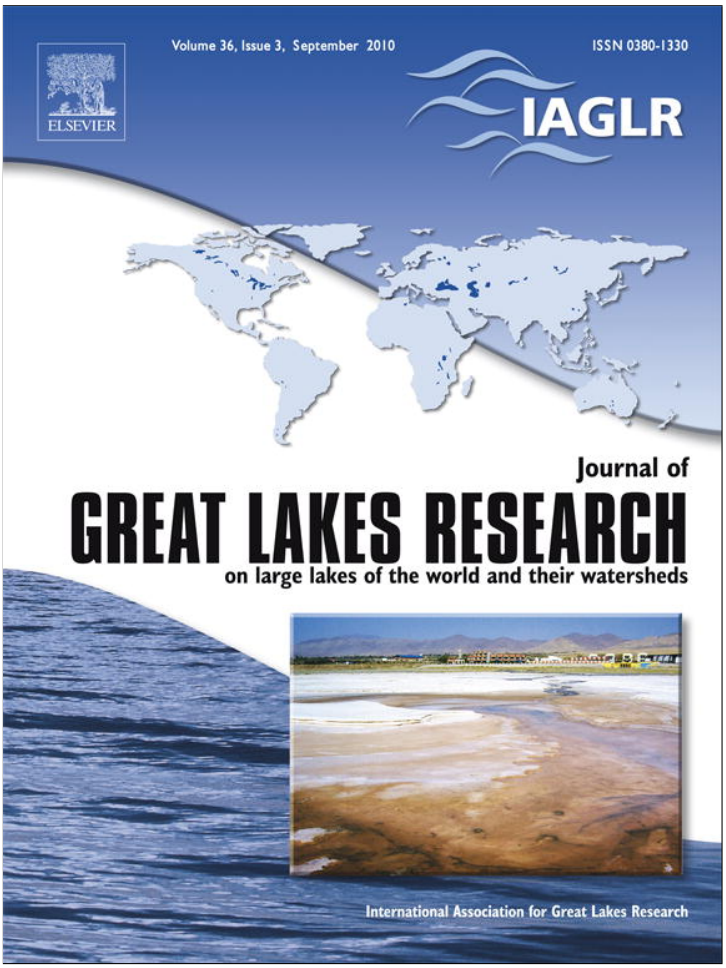

Journal of Great Lakes Research 36 (2010) 520–539

Contents lists available at ScienceDirect

Journal of Great Lakes Research

journal homepage: www.elsevier.com/locate/jglr

Eutrophication risk assessment in Hamilton Harbour: System analysis and evaluation of nutrient loading scenarios

Alex Gudimov [1], Serguei Stremilov [1], Maryam Ramin [1], George B. Arhonditsis *

Ecological Modeling Laboratory, Department of Physical & Environmental Sciences, University of Toronto, Toronto, Ontario, Canada M1C 1A4

ARTICLE INFO

Article history:
Received 6 October 2009
Accepted 11 March 2010

Communicated by Dr. Joseph DePinto

Index words:
Phosphorus loading
Eutrophication modeling
Risk assessment
Hamilton Harbour
Ecosystem restoration
Plankton dynamics

ABSTRACT

Environmental modeling has been an indispensable tool of the Hamilton Harbour restoration efforts, where a variety of data-oriented and process-based models have been used for linking management actions with potential ecosystem responses. In this study, our objective is to develop a biogeochemical model that can effectively describe the interplay among the different ecological mechanisms modulating the eutrophication problems in Hamilton Harbour, Ontario, Canada. First, we provide the rationale for the model structure adopted, the simplifications included, and the formulations used during the development phase of the model. We then present the results of a calibration exercise and examine the ability of the model to sufficiently reproduce the average observed patterns along with the major cause–effect relationships underlying the Harbour water quality conditions. The present modeling study also undertakes an estimation of the critical nutrient loads in the Harbour based on acceptable probabilities of compliance with different water quality criteria (e.g., chlorophyll a, total phosphorus). Our model suggests that the water quality goals for TP (17 μg L^{-1}) and chlorophyll a concentrations (5–10μg L^{-1}) will likely be met, if the Hamilton Harbour RAP phosphorus loading target at the level of 142 kg day^{-1} is achieved. We also provide evidence that the anticipated structural shifts of the zooplankton community will determine the restoration rate as well as the stability of the new trophic state in the Harbour.

Introduction

Hamilton Harbour, a large embayment located at the western end of Lake Ontario (Fig. 1), has a long history of eutrophication problems primarily manifested as excessive algal blooms, low water transparency, predominance of toxic cyanobacteria, and low hypolimnetic oxygen concentrations during the late summer (Charlton, 1997; Hiriart-Baer et al., 2009). Since the mid-1980s, when the Harbour was identified as one of the 43 Areas of Concern (AOC) by the Water Quality Board of the International Joint Commission, the Hamilton Harbour Remedial Action Plan (RAP) was formulated through a wide variety of government, private sector, and community participants to provide the framework for actions aimed at restoring the Harbour environment (Charlton, 2001; Hall et al., 2006). The foundation of the remedial measures originally proposed for restoring Hamilton Harbour was based on the premise that the chlorophyll concentrations and water clarity could be controlled by reducing ambient phosphorus concentrations (Environment Canada, 1981; Janus, 1987). Indeed, the substantial reduction of total phosphorus from the sewage effluents of the four wastewater treatment plants (WWTPs) and the steel mills that discharge into Hamilton Harbour, led to a significant decrease of the total phosphorus (TP) concentrations and to an improvement of the water clarity, which in turn has triggered aquatic macrophyte resurgence in most areas with Secchi disc depth greater than 3 m (Charlton and Le Sage, 1996; Charlton, 2001).

Yet, the system still receives substantial loads of phosphorus, ammonia, and suspended solids from the Burlington and Hamilton sewage treatment plants, and therefore moderate improvements in TP, chlorophyll, and total ammonia concentrations have been observed since the mid-1990s (Hiriart-Baer et al., 2009). Hamilton Harbour also experiences hypoxia in its cone-shaped hypolimnion every year during the stratification summer period, but undersaturation can also occur in winter when ice cover is extensive (Rodgers, 1998; Hiriart-Baer et al., 2009). The severity and duration of hypoxia is modulated by the thickness of the hypolimnion and the hydraulic exchanges with Lake Ontario (Barica, 1989; Hiriart-Baer et al., 2009). Aside from these natural factors, anthropogenic nutrient inputs also enhance the chemical (nitrification) and biological processes (organic matter decomposition), thereby accentuating the manifestation of hypoxia in the Harbour. Thus, although original propositions to alleviate hypoxia advocated the artificial aeration of the Hamilton Harbour hypolimnion, it was eventually deemed that the improvement of oxygen conditions through phosphorus and ammonia loading reductions would adequately control the hypolimnetic dissolved oxygen deficit (Charlton, 1993; Hamilton Harbour Technical Team—Water Quality, 2007). However, while the drastic nutrient loading reduction seems to be the way forward, the determination of the critical levels is not a straightforward issue as the

* Corresponding author. Tel.: +1 416 208 4858.
E-mail addresses: agudimov@utsc.utoronto.ca (A. Gudimov), 09stremi@utsc.utoronto.ca (S. Stremilov), maryam.ramin@utoronto.ca (M. Ramin), georgea@utsc.utoronto.ca (G.B. Arhonditsis).
[1] Tel.: +1 416 208 4878.

0380-1330/$ – see front matter © 2010 Elsevier B.V. All rights reserved.
doi:10.1016/j.jglr.2010.04.001

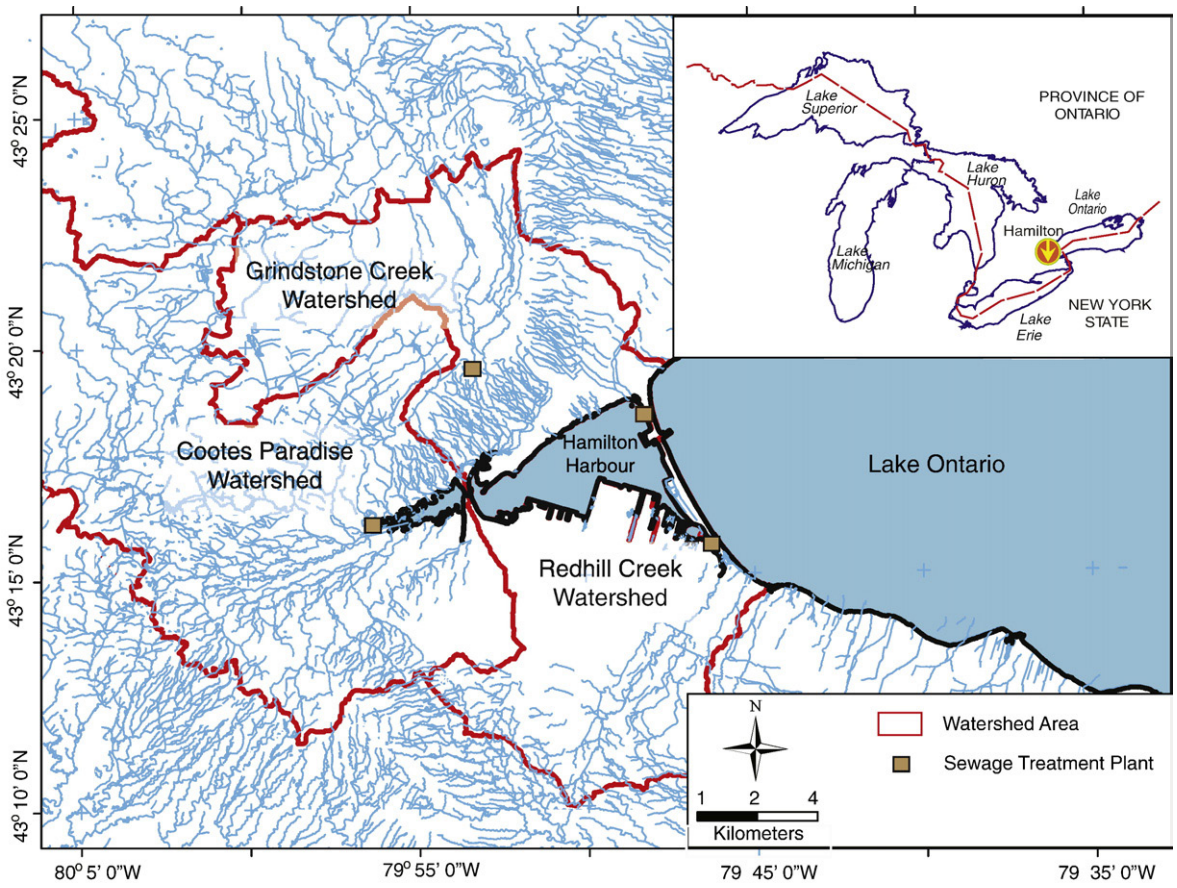

Fig. 1. Map of Hamilton Harbour, western end of Lake Ontario, with all the major point and non-point loading sources. The Red Hill Creek watershed includes the Woodward Avenue WWTP sewershed.

population growth and increasing urbanization emphasize the need for further expansion of the wastewater treatment facilities (Charlton, 1997).

The development of the most recent nutrient load reductions and the setting of water quality goals in Hamilton Harbour reflect an ecosystem-type approach that considers the complex interplay among abiotic parameters and biotic components pertinent to the beneficial uses of the Harbour (Hamilton Harbour Technical Team—Water Quality or HHTT-WQ, 2007). For example, stakeholders have selected the warm water fishery as a priority use for the Harbour which was then associated with the TP loading goals following a "mental model" that comprises a series of cause–effect relationships, i.e., fish need aquatic plants for shelter and reproduction, aquatic plants need light to grow, light will only penetrate the water column if chlorophyll *a* levels are sufficiently low, low chlorophyll *a* levels are achieved through sufficiently low TP concentrations, and low Harbour TP concentrations are a function of the total TP load to the Harbour. The next step involved the selection of target values for the exogenous nutrient loads and water quality variables that aimed to effectively integrate the environmental concerns with the local socioeconomic values. In particular, the technical team during the early stages of the RAP development had to balance among the quite variant model predictions of the Harbour conditions, the importance of different parts of the Harbour, the cost and/or feasibility of various remedial measures and different designs of the adjacent wastewater treatment plants, equity between the municipalities of Halton and Hamilton, and the varying perceptions of the stakeholders and policy makers (HHTT-WQ, 2007). Based on an analytically rigorous approach that involved data analysis, modeling, and expert judgment, the respective phosphorus loading and TP concentration targets were originally set at 142 kg/day and 17 μg/L, while the environmental goals related to chlorophyll *a* concentrations (5–10 μg/L) and Secchi disc depth (3.0 m) emerged through a consensus on what was desirable and/or achievable targets for the Harbour (Charlton, 2001). Finally, based on a recent review of the literature that evaluated the historical nature of hypolimnetic DO depletion in Hamilton Harbour, the RAP concluded that the original goal of 4 mg/L DO is unlikely to be met and that biologically meaningful and achievable DO-related targets should consider the natural state of the Harbour as well as the best cost-effective technology applied by the City of Hamilton at the Woodward Avenue WWTP (HHTT-WQ, 2007).

Environmental modeling has been an indispensable tool of the Hamilton Harbour restoration efforts, where a variety of "data-oriented" and "process-based" models have been used for examining the eutrophication goals (Snodgrass and Ng, 1985; Barica, 1989; Molot et al., 1992; McMahon and Snodgrass, 1993; Kellershohn and Tsanis, 1999). The former models are mainly steady-state, mass balance approaches that predict lake total phosphorus concentrations (TP_{lake}) as a function of lake morphometric/hydraulic characteristics, such as the areal phosphorus loading rate, mean depth, fractional phosphorus retention, and areal hydraulic loading which are then associated with the chlorophyll *a* and/or hypolimnetic DO concentrations (Ahlgren et al., 1988; Brett and Benjamin, 2008). The latter category includes models with mechanistic foundation that use ordinary or partial differential equations to describe the major aquatic biogeochemical processes (Arhonditsis and Brett, 2005a,b). However, many of the existing modeling efforts in the Hamilton Harbour have not rigorously assessed the effects of the uncertainty underlying model predictions (parametric and structural error, misspecified boundary conditions) on the projected system responses, nor has it been discussed the appropriate use of models to address percentile-based standards (Zhang and Arhonditsis, 2008). Given the substantial social and economic implications of management decisions, it is important to consider whether current water

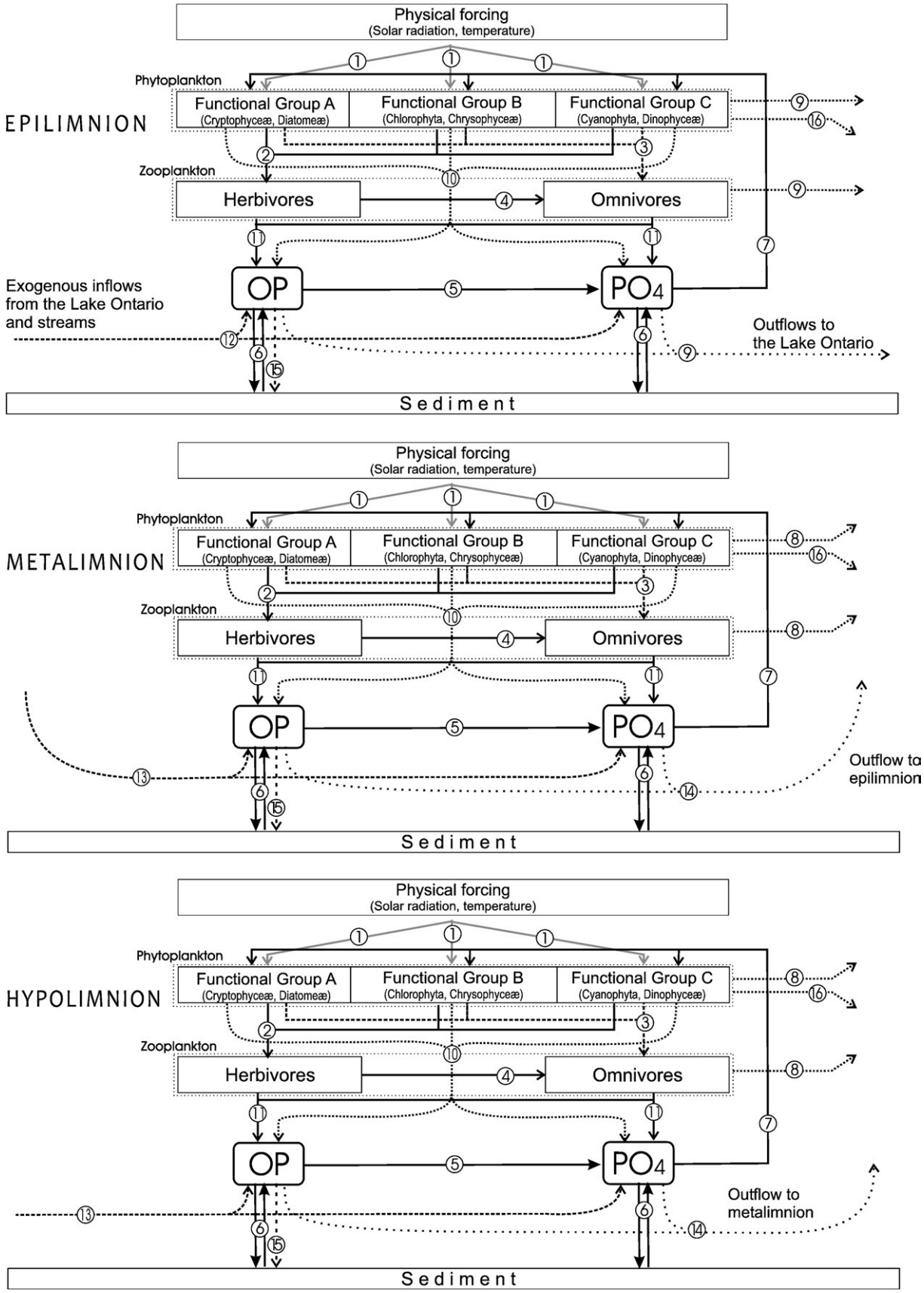

Fig. 2. The phosphorus biogeochemical cycle of the model: (1) external forcing to phytoplankton growth (temperature and solar radiation); (2) herbivorous zooplankton grazing on phytoplankton; (3) omnivorous zooplankton grazing on phytoplankton; (4) omnivorous zooplankton grazing on herbivorous zooplankton; (5) OP mineralization; (6) water–sediment exchanges of OP and PO_4 (including Fe-precipitation); (7) phosphate uptake by phytoplankton; (8) flows of plankton to upper level; (9) outflows of plankton, PO_4, and OP to the Lake Ontario; (10) phytoplankton basal metabolism excreted as PO_4 and OP; (11) zooplankton basal metabolism excreted as PO_4 and OP; (12) exogenous inflows of PO_4 and OP; (13) inflows from upper levels; (14) outflows to upper levels; (15) settling of organic particles; (16) phytoplankton settling.

quality modeling practices adequately address the type of probabilistic standards that seem to be more appropriate for complex environmental systems such as Hamilton Harbour.

In this study, our objective is to develop a biogeochemical model that can effectively depict the interplay among the different ecological mechanisms underlying the eutrophication problems in the Hamilton Harbour. First, we provide the rationale for the model structure adopted, the simplifications included, and the formulations used during the development phase of the model; the so-called *conceptual validation* (Rykiel, 1996). We then present the results of a calibration exercise and examine the ability of the model to sufficiently reproduce the average observed conditions of the Harbour along with the actual ecological processes and cause–effect relationships in the system. Several of the lessons learned during the model calibration and validation (e.g., model error, lack of data for some water quality variables, model uncertainty) are proposed to guide the refinement of the model and the future research in the Harbour. The present modeling study also undertakes an estimation of the critical nutrient loads in the Harbour based on acceptable probabilities of compliance with different water quality criteria (e.g., chlorophyll a, total phosphorus). Finally, we conclude by pinpointing the weaknesses of the conventional model "training" practices (i.e., mere adjustment of model parameters until the discrepancy between model outputs and observed data is minimized) and emphasize the importance of calibrating the same model with Bayesian inference techniques that can rigorously quantify the uncertainty associated with model structure and parameters.

Methods—model description

This section provides the description of the basic conceptual design of the model. The flow diagrams of the phosphorus and nitrogen cycles considered are depicted in Figs. 2 and 3, while the parameter definitions are presented in Appendix A. Some of the model formulations have been well documented in the modeling literature, so we will only briefly describe them. We will highlight the site-specific modifications of the model to accommodate the Hamilton Harbour plankton patterns.

Model spatial structure and forcing functions

We considered a three-compartment vertical segmentation representing the epilimnion, metalimnion (or mesolimnion), and hypolimnion of the Harbour (Fig. 4). The depths of the three boxes were explicitly defined based on extensive field measurements for the study period 1987–2007 (Dermott et al., 2007; Hiriart-Baer et al., 2009). The epilimnion corresponds to the maximum depth where the water temperature varied ≤ 1 °C relative to the temperature at 0.5 m during the summer stratified period in the system and was set equal to 8 m. An equal box-depth was assigned to mesolimnion, which represented the transient area in the water column between epilimnion and hypolimnion. Seasonally varying mass exchanges among the three compartments were computed using Fick's Law (Klapwijk and Snodgrass, 1985; Hamblin and He, 2003). Other external forcing functions include the solar radiation, day length, precipitation, and evaporation based on meteorological data from Environment Canada, namely, the Canadian Daily Climate Data (1996–2002) and the Canadian Climate Normals (1971–2000) (http://www.climate.weatheroffice.ec.gc.ca/prods_servs/index_e.html). Loads of inorganic nutrients and organic matter enter the Hamilton Harbour from the following main sources: Red Hill and Grindstone creeks, combined sewer overflows (CSOs), Dofasco and Stelco steel mills, Woodward and Skyway wastewater treatment plants (WWTPs), and Cootes Paradise. Estimates of flow and nutrient loadings are based on available data from the Water Survey of Canada (http://www.wsc.ec.gc.ca/) and the RAP loading report (Hamilton Harbour Technical Team: 1996–2002 Contaminant Loadings and Concentrations to Hamilton Harbour or HHTT-CLR, 2004). Similar to the practice followed by Arhonditsis and Brett (2005a,b), the model was run with the mean hydrological and nutrient loading annual cycle over the 1996–2002 period.

The exchanges between Hamilton Harbour and the relatively high quality waters of Lake Ontario through the Burlington Ship Canal are another major influence on Harbour water quality resulting in the dilution of pollutant concentrations, the reduction of the Harbour's residence time, and the oxygenation of the hypolimnetic waters (Barica, 1989; Hamblin and He, 2003). In particular, the winter exchanges are primarily driven by short-term oscillations due to water level differences at the two ends of the canal, while the exchanges during the summer stratified period are mediated by slowly fluctuating density gradients, i.e., warm Harbour water flowing to the lake in the top layer and colder lake water flowing to the Harbour in the bottom layer (see Figs. 1 and 2 in Barica, 1989). Moreover, existing evidence also suggests that the Hamilton Harbour-Lake Ontario interplay during the stratified conditions is much stronger and steadier than the winter period (Hamblin and He, 2003). In this study, following the Klapwijk and Snodgrass (1985; see their Fig. 3) conceptual model, we assumed that 20% of the Lake Ontario inflows are directly discharged to the epi- and mesolimnion, whereas 80% of the fresher oxygenated lake water replaces the hypolimnetic masses in the Harbour.

Equations

We developed an ecological model that considers the interactions among the following state variables: nitrate, ammonium, organic nitrogen, phosphate, organic phosphorus, three phytoplankton, and two zooplankton functional groups.

Phytoplankton

A detailed description of the current phytoplankton seasonal succession patterns in Hamilton Harbour was presented by Munawar and Fitzpatrick (2007). Briefly, the phytoplankton community primarily consists of chlorophytes, diatoms, cryptophytes, and dinophytes which dominate the system during different periods of the annual cycle. The physical conditions become more favorable (day length increase, solar warming, ice melt, and shallowing of the mixed layer) around the end of April to early May, stimulating the phytoplankton growth. The timing and the maximum levels of the spring phytoplankton biomass are characterized by significant interannual variability and are somewhat unclear, partly due to the fact that the sampling cruises of the local monitoring programs typically do not start before the first or second week of May, a period that may coincide with the recession rather than the peak of the spring bloom (see also following discussion). The spring phytoplankton community is overwhelmingly dominated (>80%) by diatoms (*Fragilaria crotonensis*, *Stephanodiscus niagarae*) and cryptophytes (*Rhodomonas minuta*, *Cryptomonas reflexa*), while dinophytes (*Gymnodinium helveticum*, *Ceratium furcoides*), chrysophytes (*Ochromonas* sp., *Dinobryon divergens*), and chlorophytes (*Coenochloris pyrenoidosa*, *Scenedesmus braziliensis*, *Coelastrum reticulatum*) may also be observed in relatively low levels (Munawar and Fitzpatrick, 2007). During the summer stratified period, the phytoplankton biomass is subject to frequent "wax and wane" cycles around the level of 15 μg chlα L^{-1} (Hiriart-Baer et al., 2009). The phytoplankton community is typically composed of chlorophytes in the early to mid-summer period, whereas cryptophytes and dinophytes become more prevalent in the late summer period. The cyanobacteria (*Aphanizomenon* sp., *Microcystis* sp., *Lyngbya birgei*) levels remain relatively low until mid-August, when they can account for up to 20–25% of the total phytoplankton biomass. In early fall, the phytoplankton community is usually dominated by dinophytes followed by a mixture of chlorophytes, diatoms, and cryptophytes later in the fall. Munawar and Fitzpatrick (2007) also noted that the phytoplankton succession patterns and especially the summer phytoplankton community composition can be highly variable,

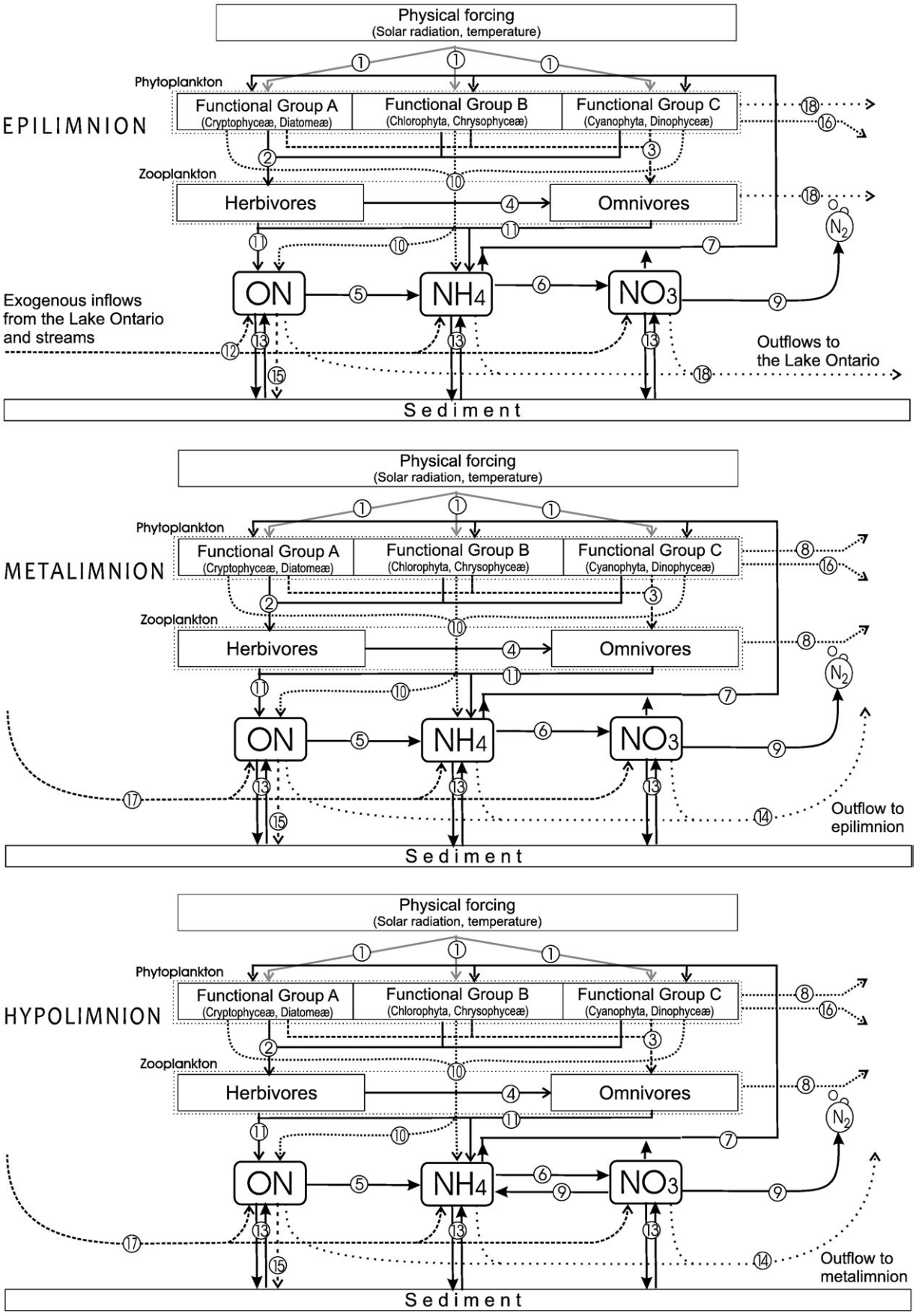

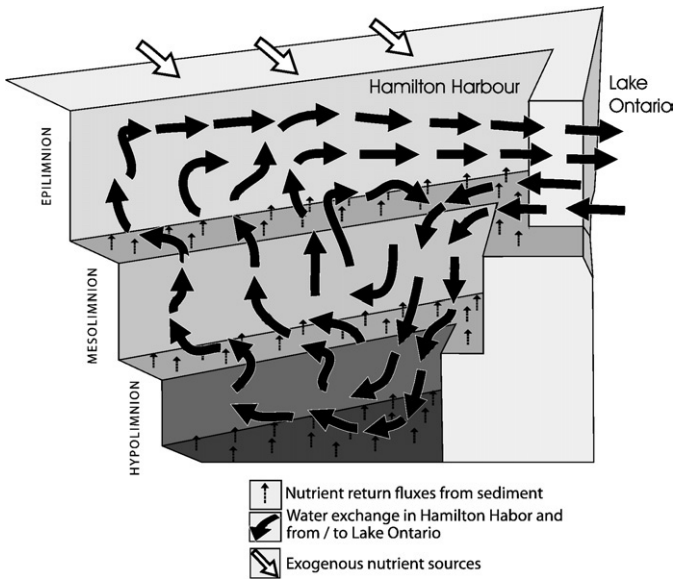

Fig. 4. Spatial segmentation of the Hamilton Harbour eutrophication model.

mainly driven by the frequent extreme physical disturbances in the Harbour such as ship traffic, wind, and storm events.

The ecological submodel simulates three phytoplankton functional groups that differ with respect to their strategies for resource competition (nitrogen, phosphorus, light, and temperature) and metabolic rates as well as their morphological features (settling velocities, self-shading effects) and edibility for zooplankton. The functional group A (PFG A) has attributes of r-selected organisms with high maximum growth rates and higher metabolic losses, strong phosphorus and weak nitrogen kinetics, lower tolerance to low light availability, low temperature optima, and high sinking velocities as well as high palatability as food source for zooplankton. Thus, although this group primarily aims to reproduce the dynamics of the spring diatom-dominated phytoplankton community, the high-edibility feature assigned may indirectly reflect the functional role that cryptophytes play in the system (Brett et al., 2000). Following the classification scheme presented by Arhonditsis et al. (2007), we consider a second functional group (PFG C) modeled as K-strategists with low maximum growth and metabolic rates, weak phosphorus and strong nitrogen competition abilities, higher tolerance to low light availability, low settling velocities, high temperature optima, and low edibility. The specification of this group aims to adequately describe the dynamics of the majority species of Cyanophyta and Dinophyceae observed in the Harbour. The third assemblage (labelled as PFG B) was parameterized so that the average functional properties assigned resemble to those of other major residents of the summer phytoplankton community (chlorophytes, chrysophytes), thereby providing an intermediate competitor that more realistically depicts the continuum between diatom- and cyanobacteria-dominated communities.

The governing equation for phytoplankton biomass accounts for phytoplankton production and losses due to mortality, settling, dreissenid filtration, and herbivorous zooplankton grazing. The phytoplankton growth is controlled by the water temperature conditions as well as the nutrient and light availability. Phytoplankton growth temperature dependence has an optimum level (T_{opt}) and is modeled by a function similar to Gaussian probability curve (Cerco and Cole, 1993; Arhonditsis and Brett, 2005a,b). Phosphorus dynamics within the phytoplankton cells account for luxury uptake, i.e., phytoplankton nutrient uptake depends on both internal and external concentrations confined by upper and lower internal levels (Hamilton and Schladow, 1997; Arhonditsis et al., 2002). Our model explicitly considers the role of new and regenerated production using separate formulations that relate phytoplankton uptake to the ambient nitrate and ammonium concentrations (Eppley–Peterson *f*-ratio paradigm; Eppley and Peterson, 1979). Regarding the dependence of photosynthesis on solar radiation, we used Steele's equation along with Beer's law to scale photosynthetically active radiation to depth. The extinction coefficient is determined as the sum of the background light attenuation and attenuation due to chlorophyll *a* (Jassby and Platt, 1976). The former coefficient coupled with a piecewise approach was also used to reproduce the illumination of the water column during the ice-covered period (Huber et al., 2008). The phytoplankton mortality includes all internal processes that decrease algal biomass (respiration, excretion) as well as natural mortality and is assumed to increase exponentially with temperature. Phytoplankton settling considers the net change in biomass due to settling between adjacent compartments. We also incorporated a first-order loss rate representing the filtration from the zebra and quagga mussels, which can be a potentially important factor for the phytoplankton biomass levels; especially in nearshore areas (Bierman et al., 2005).

Zooplankton

Despite the spatiotemporal variability characterizing the Hamilton Harbour zooplankton community, Gerlofsma et al. (2007) noted a structural shift to a more diverse community less dominated by rotifers, which in turn may reflect an improvement of the integrity of the food web structure, and increase in the energy flow to higher trophic levels. However, the present zooplankton community still indicates that Hamilton Harbour is eutrophic, being dominated by cladocerans and cyclopoids (*Diacyclops thomasi*, *Cyclops vernalis*) compared to calanoids (*Leptodiaptomus siciloides*). Cladocerans mainly include the *Bosmina longirostris,* species from the *Daphnia* and *Ceriodaphnia* genera, and the carnivorous species *Leptodora kindtii* and *Cercopagis pengoi.* The proportion of carnivorous to herbivorous zooplankton is relatively high in the Harbour, typically accounting for 25–50% of the zooplankton biomass. Gerlofsma et al. (2007) interpreted this pattern as evidence that the standing phytoplankton biomass can sufficiently support large biomass of herbivorous zooplankton, which in turn supports a large carnivorous zooplankton biomass. The present model simulates two zooplankton functional groups, which primarily differ with regards to their feeding strategies aiming to represent the herbivorous and omnivorous zooplankton community in the Harbour.

Zooplankton grazing and losses due to natural mortality/consumption by higher predators are the main two terms in the zooplankton biomass equation. Herbivorous zooplankton has four alternative food sources (the three phytoplankton groups and the biogenic particulate material or detritus) grazed with preference that changes dynamically as a function of their relative proportion (Fasham et al., 1990). The present model parameterization also postulates a selective zooplankton preference for the assemblages PFG A, PFG B, and detritus over cyanobacteria. Omnivorous zooplankton feeds upon herbivorous zooplankton but its diet also depends on the relative abundance of the rest of the food sources in the system. Holling's type II functional response was used to model the temperature-dependent zooplankton grazing and the assimilated fraction of the grazed material fuels growth. In the absence of information to support more complex forms, we selected a linear closure term that represents the effects of a seasonally invariant predator biomass (see Edwards and Yool, 2000).

Fig. 3. The nitrogen biogeochemical cycle of the model: (1) external forcing to phytoplankton growth (temperature, solar radiation); (2) herbivorous zooplankton grazing on phytoplankton; (3) omnivorous zooplankton grazing on phytoplankton; (4) omnivorous zooplankton grazing on herbivorous zooplankton; (5) ON mineralization; (6) nitrification; (7) phytoplankton uptake; (8) outflows of plankton to upper level; (9) NO_3 sinks due to denitrification; (10) phytoplankton basal metabolism excreted as NH_4 and ON; (11) zooplankton basal metabolism excreted as NH_4 and ON; (12) exogenous inflows of NO_3, NH_4, and ON; (13) water–sediment NO_3, NH_4 and ON exchanges; (14) outflow to upper levels; (15) settling of organic particles; (16) phytoplankton settling; (17) inflows from upper levels; (18) outflows of NO_3, NH_4, and ON, and plankton to the Lake Ontario.

Phosphorus cycle

Two state variables of the phosphorus cycle are considered in the model: phosphate (PO_4) and organic phosphorus (OP) (Fig. 2). The phosphate equation considers the phytoplankton uptake, the proportion of phytoplankton and zooplankton mortality/higher predation that is directly supplied into the system in inorganic form, the bacteria-mediated mineralization of organic phosphorus, and the net diffusive fluxes among the three spatial compartments. We also accounted for the phosphorus precipitated to the sediment due to iron loadings from the two steel mills, based on an empirical equation originally implemented to correct for the observed Hamilton Harbour phosphorus concentrations (HHTT-WQ, 2007). The organic phosphorus equation also considers the amount of organic phosphorus that is redistributed through phytoplankton and zooplankton basal metabolism. A fraction of organic phosphorus settles to the sediment and another fraction is mineralized to phosphate through a first-order reaction. We also consider external phosphorus loads to the system and losses via the exchanges with Lake Ontario.

Nitrogen cycle

There are three nitrogen forms considered in the model: nitrate (NO_3), total ammonia (NH_3), and organic nitrogen (ON) (Fig. 3). The ammonia equation considers the phytoplankton uptake and the proportion of phytoplankton and zooplankton mortality that is returned back to the system as ammonium ions. Ammonia is also oxidized to nitrate through nitrification, and the kinetics of this process is modeled as a function of the ammonia, dissolved oxygen, temperature, and light availability (Cerco and Cole, 1993; Tian et al., 2001). We used Wroblewski's (1977) model to describe ammonia inhibition of nitrate uptake. The nitrate equation also takes into account the amount of ammonia oxidized to nitrate through nitrification and the amount of nitrate lost as nitrogen gas through denitrification. The latter process is modeled as a function of dissolved oxygen, temperature, and the contemporary nitrate concentrations (Arhonditsis and Brett, 2005a). The organic nitrogen equation considers the contribution of phytoplankton and zooplankton mortality to the organic nitrogen pool and the seasonally forced bacterial mineralization that transforms organic nitrogen to ammonia. External nitrogen loads to the system and losses via the exchanges with Lake Ontario are also included.

Fluxes from the sediment

As a first approximation to model the role of the sediments, we followed a simple dynamic approach that relates the fluxes of nitrogen and phosphorus from the sediment with the algal and particulate matter sedimentation and burial rates while also accounting for the role of temperature (Arhonditsis and Brett, 2005a). The relative magnitudes of ammonium and nitrate fluxes were also determined by nitrification and denitrification occurring at the sediment surface.

Results and discussion

Sensitivity analysis

We conducted a local sensitivity analysis to identify the most influential parameters for all the major model endpoints of management interest (nutrient concentrations, phytoplankton abundance, zooplankton biomass). The procedure followed was based upon 40,000 sets sampled from a zone of the parameter space that was centered on the final model solution (calibration vector in Appendix A). In particular, the model parameters were sampled independently from Gaussian distributions with mean values derived from the calibration exercise and standard deviations that were set equal to the 10% of the parameter values. Similar to the Arhonditsis and Brett (2005a) protocol, we developed multiple regression models for the phosphate, total phosphorus, nitrate, ammonia, total nitrogen, chlorophyll *a* summer epilimnetic averages (June–September), and the total herbivorous/omnivorous zooplankton biomass summer averages weighted over the epilimnion, mesolimnion, and hypolimnion of the Harbour (Table 1). In all cases, the model r^2-values were high (>0.85) which indicates that within the selected setting (e.g., parameter ranges, average external nutrient loading conditions) the relationship between the input parameters and model outputs can be approximated as linear and that the system does not reach its carrying capacity (see also the uncertainty bounds delineated by the black lines in Fig. S1 in the Electronic Supplementary Material). Based on the values of the semi-partial coefficients of determination (r^2_{spart}), we found that the most influential parameter for phosphate, total phosphorus, and chlorophyll *a* concentrations is the fraction of inert phosphorus buried into deeper sediment (β_P), accounting for 26.5%, 56.8%, and 26.0% of the variability associated with the corresponding model outputs. The epilimnetic phosphate levels were positively related to the maximum grazing rates ($maxgrazing_j$) of herbivorous (19.5%) and omnivorous (7.6%) zooplankton, reflecting their importance in regulating zooplankton's ability to crop the standing phytoplankton biomass and thus the amount of dissolved-phase phosphorus being utilized. Evidence of the importance of the same causal connection is also provided by the negative relationship between epilimnetic phosphate and the zooplankton mortality rates ($mz_{j,j=herb,omni}$). The specification of the two zooplankton groups (maximum grazing rates, mortality rates) also appears to shape the summer epilimnetic total phosphorus and chlorophyll *a* concentrations. We also note the important role of the

Table 1
Sensitivity analysis results of the Hamilton Harbour eutrophication model.

Epilimnetic phosphate (0.856)	r^2_{spart}	Epilimnetic total phosphorus (0.977)	r^2_{spart}	Epilimnetic chlα (0.887)	r^2_{spart}	Herbivorous zooplankton (0.958)[a]	r^2_{spart}
β_P[b]	0.265	β_P[b]	0.568	β_P[b]	0.260	$maxgrazing_{herb}$[b]	0.253
$maxgrazing_{omni}$	0.195	$V_{settling}$[b]	0.317	$maxgrazing_{omni}$[b]	0.188	$maxgrazing_{omni}$[b]	0.234
mz_{omni}[b]	0.136	mz_{omni}	0.021	mz_{omni}	0.153	mz_{herb}[b]	0.232
$maxgrazing_{herb}$	0.076	$maxgrazing_{omni}$[b]	0.020	$maxgrazing_{herb}$[b]	0.071	mz_{omni}	0.144
mz_{herb}[b]	0.044	$maxgrazing_{herb}$[b]	0.014	mz_{herb}	0.054	Kz_{omni}	0.023
Omnivorous zooplankton (0.962)[a]	**r^2_{spart}**	**Epilimnetic total nitrogen (0.983)**	**r^2_{spart}**	**Epilimnetic nitrate (0.985)**	**r^2_{spart}**	**Epilimnetic ammonia (0.976)**	**r^2_{spart}**
$maxgrazing_{omni}$	0.344	$gwthmax_{PFGA}$[b]	0.203	$gwthmax_{PFGA}$[b]	0.176	$gwthmax_{PFGB}$[b]	0.147
mz_{omni}[b]	0.333	$gwthmax_{PFGB}$[b]	0.158	$gwthmax_{PFGB}$[b]	0.157	$AH_{PFG\ A}$	0.124
$maxgrazing_{herb}$[b]	0.086	$Kextchla_{PFGA}$	0.097	$Kextchla_{PFGA}$	0.094	$AH_{PFG\ B}$	0.094
mz_{herb}	0.046	$Kextchla_{PFGC}$	0.085	β_P	0.088	$gwthmax_{PFGA}$[b]	0.090
Kz_{omni}[b]	0.035	$Kextchla_{PFGB}$	0.084	$Kextchla_{PFGC}$	0.083	$gwthmax_{PFGC}$[b]	0.078

Ranking was based on the values of squared semi-partial coefficients (r^2_{spart}) for the averages of the water quality variables during the summer stratified period. The parentheses indicate the r^2 values of the respective multiple regression models ($n = 40{,}000$).

[a] Based on weighted averages over the epilimnion, metalimnion, and hypolimnion of the Harbour.

[b] Negative sign of the regression coefficients.

values assigned to the allochthonous particle settling velocity ($V_{settling}$), $r^2_{spart} = 0.317$, in determining the levels of total phosphorus in the Harbour epilimnion. The intricate relationship between herbivorous and omnivorous zooplankton, partly predatory and partly competitive for the same food sources (phytoplankton, detritus), is primarily regulated by the relative values assigned to their grazing and metabolic capacities ($maxgrazing_j$, KZ_j, $mz_{j,\ j=herb,omni}$). The maximum growth rates ($gwthmax_{i,\ i=PFG\ A,\ PFG\ B,\ PFG\ C}$) of the three phytoplankton functional groups are particularly influential on the epilimnetic nitrogen concentrations, whereas their light attenuation coefficients ($Kextchl\alpha_{i,i=PFG\ A,\ PFG\ B,\ PFG\ C}$) appear to be important for the total nitrogen and nitrate levels. The half saturation constants for ammonia uptake (AH) of the two more abundant functional groups (i.e., PFG A and PFG B) in the summer phytoplankton community can significantly control the epilimnetic ammonia levels, despite their inferior nitrogen kinetics (Appendix A). Finally, we examined the sensitivity of the model predictions to the specification of the boundary conditions associated with the Lake Ontario water quality characteristics. Using a similar Monte Carlo approach, we found that the corresponding perturbations induce substantial variability into the simulated system dynamics (Fig. S2). However, aside from the positive relationship between the Lake Ontario zooplankton biomass and the corresponding predictions in the system, none of the other model endpoints was characterized by a systematic trend.

Model predictions and observed Hamilton Harbour dynamics

This section presents the results from a calibration exercise that mainly aimed to serve as an exploratory analysis of the model as well as an opportunity to gain insights into the simulated epilimnetic phosphorus and nitrogen cycles during the summer stratified period. Similar to the Arhonditsis and Brett (2005b) practice, our calibration was focused on the model ability to realistically reproduce the recent average water quality conditions along with the actual ecological processes and cause–effect relationships that underlie the Harbour dynamics (Dermott et al., 2007; Hiriart-Baer et al., 2009). The selection of a calibration scheme that is framed upon the average patterns rather than the year-to-year variations is directly related to the credibility of the loading estimates in the system. The existing calculations of the exogenous loadings are based on unfounded assumptions (e.g., a piecewise monotonic increase of the nutrient concentrations with the flow rates) and limited information about the seasonal variability (HHTT-CLR, 2004). Consequently, a calibration exercise focused on several years would have entailed finding an ecological parameterization that effectively links a highly uncertain forcing function (year-specific nutrient loading) to the ambient water quality conditions for a particular period. Given that there is also no reliable information to validate the model, this calibration practice is unlikely to identify a model solution that gives "good results" for the "right reasons"! Rather, we adopted a more conservative strategy that uses a model forced with the average (and thus more reliable) loading conditions to reproduce the average planktonic patterns in the Harbour. Thus, our calibration strategy is just a matter of confidence on the model inputs and an attempt to minimize the likelihood of getting good fit to the observed data by introducing a series of errors that cancel each other out.

The discrepancy between model outputs and observed monthly averages from 1997 to 2007 was assessed by calculating the coefficient of determination (r^2) and the relative error (RE) values (Fig. 5). In Fig. S1, we also illustrate the model performance combined with the 95% uncertainty bounds that depict the propagation of the variability associated with the exogenous nutrient loading through the model (see also Fig. 6). Generally, the model accurately reproduces the average PO_4, TP, NO_3, NH_3, TN, chlorophyll *a*, and total zooplankton biomass patterns. In particular, the model accurately predicts the winter maxima ($\approx$11.5 μg/L) and the summer minima ($\approx$2.2–3.5 μg/L) of the epilimnetic phosphate levels as well as the hypolimnetic accumulation during the summer stratified period ($\approx$4.2–6.5 μg/L). The latter pattern is primarily driven by the interplay between the Lake Ontario inflows and the phosphorus sediment fluxes, while the parameterization presented in Appendix A implies phosphorus release rates from the sediment within the range of 1.2–1.5 mg/m^2/day. By contrast, Mayer and Manning (1990) and later the Kellershohn and Tsanis (1999) study suggested that the phosphorus release is fairly minimal even during periods of prolonged hypoxia in the Hamilton Harbour. This absence of release was mainly attributed to high iron concentrations within sediments which reduced the bioavailability of phosphorus. Moreover, the redox potential of the sediment–water interface is surmised to be sufficiently low to allow denitrification and the release of manganese, but not low enough to allow the release of phosphorus (MOE, 1985). The discrepancy between our estimate and those reported from other field and modeling studies invites investigation to further elucidate the role of the sediment on the intra- and interannual Harbour variability of phosphate concentrations in the water column. The model accurately predicts the epilimnetic total phosphorus levels (28–35 μg/L) but seems to underpredict somewhat the hypolimnetic total phosphorus concentrations. Namely, our model provides evidence that total phosphorus drops below the 25-μg/L value in the Harbour hypolimnion, which is lower than the seasonal geometric mean of 25.4 μg/L reported by Hiriart-Baer et al. (2009). It should be noted though that the latter value is calculated over the 1987–2007 period and may not reflect the contemporary hypolimnetic total phosphorus levels.

Because the model does not accurately capture the seasonal variability of the ammonia concentrations, the relative error associated with the corresponding model predictions was quite high (RE$\approx$60%). Moreover, the current calibration vector predicts an ammonium release from the sediment within the 45- to 50-mg/m^2/day range. This estimate is significantly lower compared to the Kellershohn and Tsanis (1999) predictions (300 mg/m^2/day) but is remarkably close to the sediment fluxes reported by Van Arkel (1993) for the year 1977. Nitrate/nitrite concentrations are increasing rapidly and have been increasing at an exponential rate for almost four decades in the Harbour (Barica, 1989). While concentrations are well below the Canadian Water Quality Guideline of 13 mg/L, their implications in the ecosystem functioning remain to be assessed (Hiriart-Baer et al., 2009). In this study, we found significant agreement between predicted and observed winter and spring nitrate concentrations, but the model seems to underestimate the summer epi- and hypolimnetic levels. Aside from the assigned nitrification rates in the water column and/or the sediments (see following discussion), one plausible explanation may be the substantial uncertainty associated with the exogenous loading estimates, as we are lacking reliable information with regards to the nitrate/nitrite concentrations in all the major point and non-point sources, especially after the upgrading of the nitrification facilities in the local wastewater treatment plants. According to the model predictions, the total nitrogen concentrations can reach the level of 3–4 mg/L during the winter and fall down to 1.5 mg/L during the summer stratified period. These predictions, however, are quite uncertain given that we are lacking total nitrogen data from both the exogenous sources and the receiving water body. Generally, the substantial uncertainty associated with the reproduction of the nitrogen cycle underscores the need of improving our contemporary understanding of the underlying processes in the system, and this information can be subsequently used to further refine the model parameterization.

The model closely reproduces the winter ($\approx$5 μg chlα/L) and the summer ($\approx$15–20 μg chlα/L) phytoplankton levels, but seems to overpredict the spring chlorophyll *a* concentrations in that the model predicts a major spring phytoplankton bloom exceeding the level of 20 μg chlα/L. This discrepancy in regards to the Harbour phenology may stem from the absence of reliable information from the system (Hiriart-Baer et al., 2009), as the sampling cruises of the local monitoring programs typically do not start before the first or second week of May, a period that may coincide with the recession rather than the peak of the

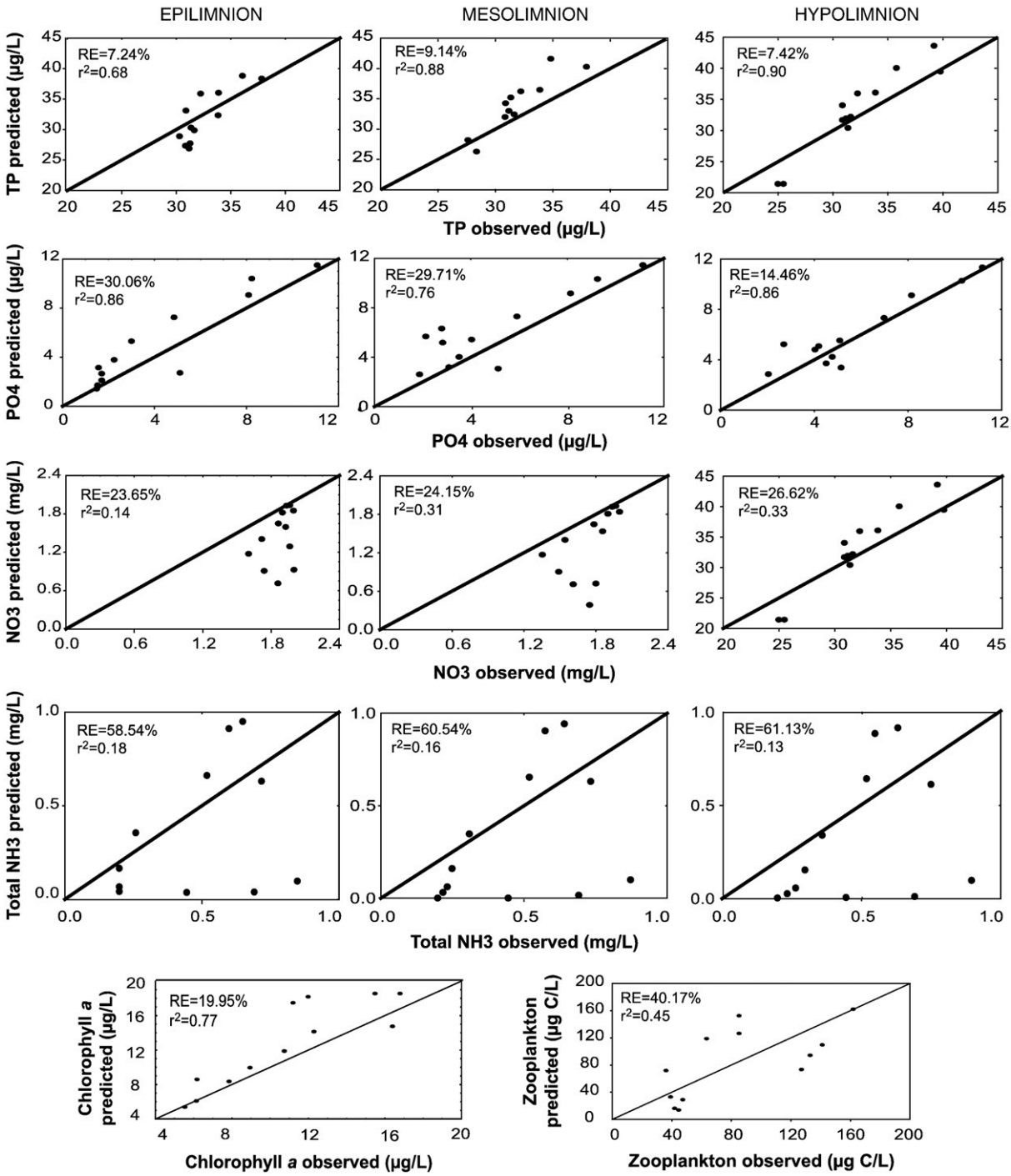

Fig. 5. Comparison between simulated and observed values for the Hamilton Harbour epilimnion, metalimnion, and hypolimnion (r^2: coefficient of determination; RE: relative error). The diamond dots correspond to the mean observed values in Hamilton Harbour from 1997 to 2007.

spring bloom. According to the model predictions, the average epilimnetic primary productivity rate at optimal irradiance levels is approximately 47 mg C/m^3/h during the summer season, which falls within the 36- to 75-mg C/m^3/h range reported by Munawar and Fitzpatrick (2007). Under the present (or more extreme) nutrient loading conditions, the phytoplankton succession patterns predicted by the model are very close to the ones typically reported in Hamilton Harbour (Munawar and Fitzpatrick, 2007). During the spring bloom, the functional group A (diatoms, cryptophytes) dominates the phytoplankton community (45% of the total phytoplankton biomass), while the functional groups B (chlorophytes, chrysophytes) and C (cyanobacteria, dinoflagellates) account for approximately 35% and 25%, respectively. By contrast, the summer phytoplankton community is divided almost equally between the three functional groups. Notably, aside from the decrease of the total phytoplankton biomass, our model also predicts that the gradual decrease of the nutrient loading will also decrease the *PFG C* contribution to the summer phytoplankton community by 5–10% (Fig. 7).

Our model also predicts two major peaks of the total zooplankton biomass (Fig. 7 and Fig. S1); the first peak follows the spring phytoplankton bloom (≈200 µg C/L) while the second one is predicted to occur at the end of summer-early fall (≈180 µg C/L). These predictions match closely the observed patterns reported by Munawar and Fitzpatrick (2007), e.g., Figs. 8 and 9, pp. 62–63, if we assume an

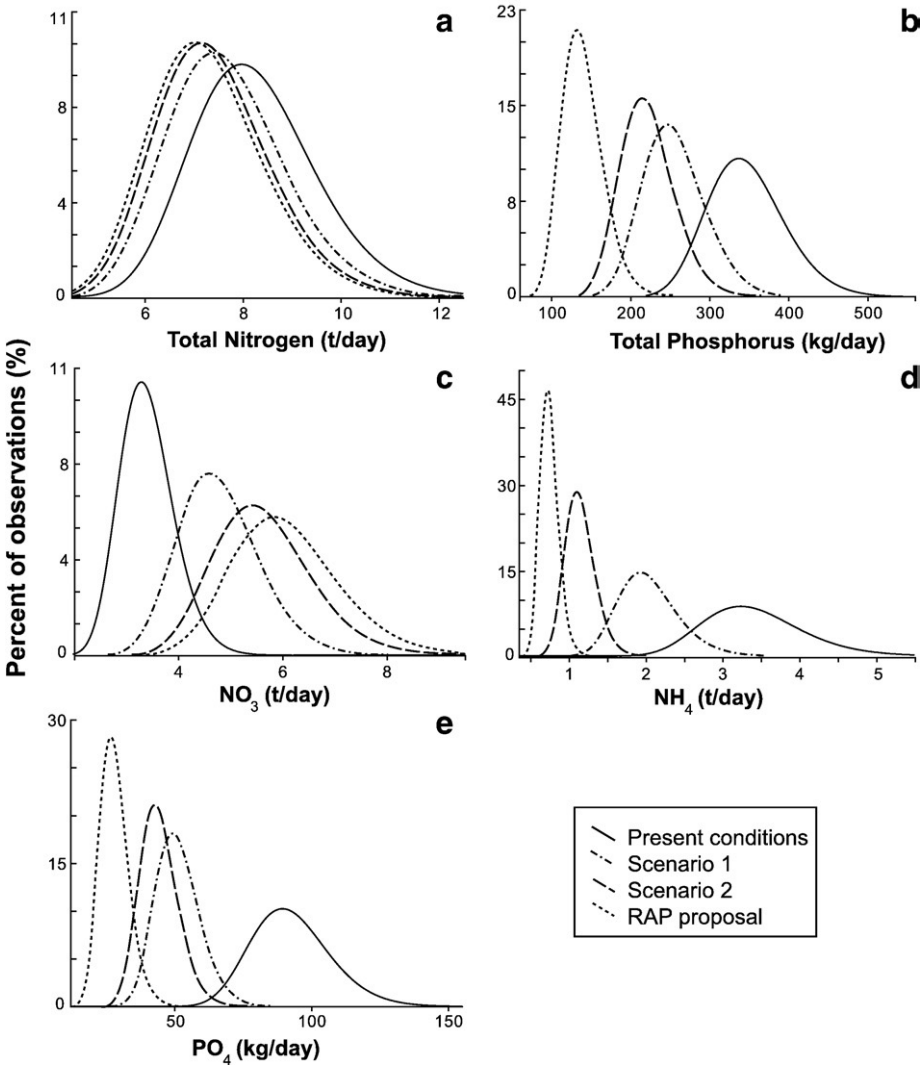

Fig. 6. Analysis of scenarios: distributions of the exogenous nutrient loadings used to force the Hamilton Harbour eutrophication model.

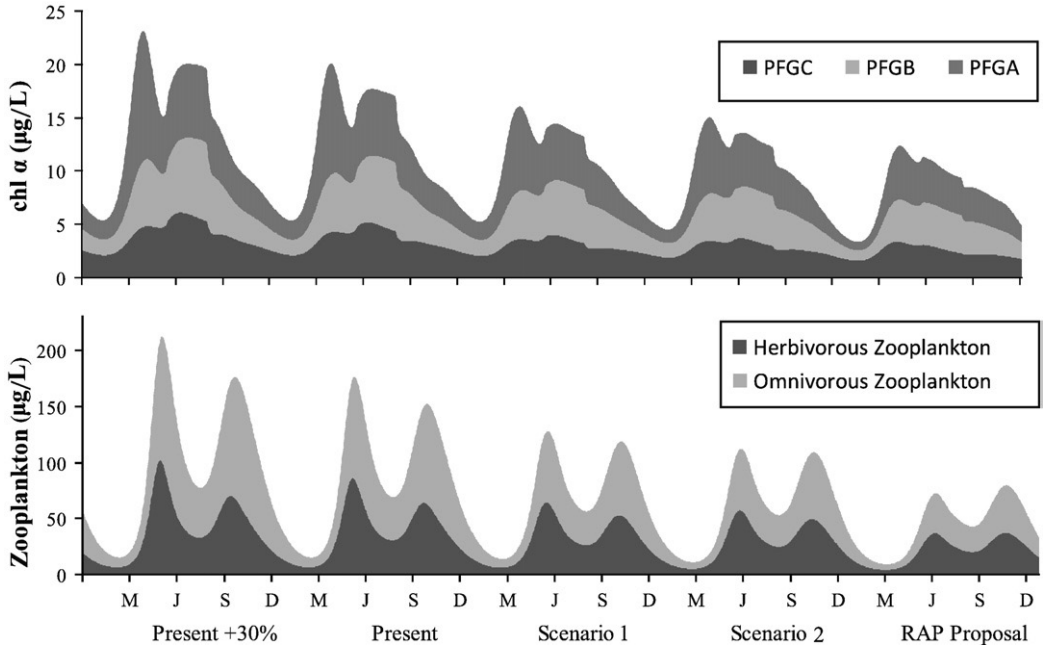

Fig. 7. Simulated seasonal phytoplankton and zooplankton succession patterns under five exogenous nutrient loading conditions.

average wet to dry biomass ratio equal to 10 along with 0.4 μg C per μg of dry zooplankton biomass (Downing and Rigler, 1984). Similar to the observed patterns, the simulated proportion of omnivorous to herbivorous zooplankton varies between 25% and 50% during the seasonal cycle (Fig. 7). Based on the assigned preferences, relative abundances, and assimilation rates, herbivorous zooplankton primarily feed upon the functional group A (≈50%) and secondarily upon the second functional group and detritus (20–25% each food source), while the third functional group consistently accounts for less than 10% of their diet. Similarly, the omnivorous zooplankton feeding patterns rely on phytoplankton and detritus, although herbivorous zooplankton contributes up to 10% of their diet. Given the high value assigned to the parameter $Pref_{omniherb}$, the predominance of phytoplankton on the omnivores' diet is probably surprising and should be attributed to the formula used in our model that weights the nominal preferences with the relative abundance of the different food types.

System dynamics—analysis of scenarios

For the purpose of reproducing the broad range of dynamics experienced in Hamilton Harbour, we formulated probability distributions to accommodate the uncertainty as well as the interannual variability associated with the different exogenous nutrient loading sources (Fig. 6; see also Tables S1–S4). From the three WWTPs located in the City of Hamilton, our analysis explicitly considers the discharges from the Woodward WWTP, whereas the effluents from the Dundas and Waterdown WWTPs are captured by the Cootes Paradise and Grindstone Creek nutrient loadings, respectively. The average TP loading used to represent the present Woodward WWTP discharges was 194.2 kg/day stemming from an approximate flow of 343 megalitres per day and a concentration of 0.568 mg TP/L (Table 2). The 2.5% and 97.5% uncertainty bounds of the TP loadings examined were 127.2 and 278.8 kg/day. The TP discharges from the same WWTP were reduced by 20% (155 kg/day) and 38% (120 kg/day) in scenarios 1 and 2, until set equal to the final goal of 60 kg/day or 70% reduction as per the Hamilton Harbour RAP recommendations (HHTT-CLR, 2004). Similarly, the NH_3 loading from this source was reduced by 40% (1800 kg/day), 70% (900 kg/day), and 82% (530 kg/day) relative to the present levels (3023.6 kg/day), while the assumption of an equivalent NO_3 loading increase aims to represent the hypothetical scenario of enhanced nitrification in the WWTP (Table 2). The role of the Burlington Skyway WWTP was examined assuming average loadings of 20.4 kg TP/day and 155.9 kg NH_3/day (present conditions) and ending up with 12 kg TP/day and 115 kg NH_3/day under the HH RAP proposition. Cootes Paradise, a large wetland at the western end of the system, is another major nutrient loading source to the Hamilton Harbour. In this study, the nutrient loadings encompass the discharges from the Dundas WWTP and the Spencer, Borer, Chedoke, and Ancaster Creeks based on a steady-state assumption that the inflows entering Cootes are equal to the flows out to Hamilton Harbour. Starting from an average of 40.8 kg/day, the TP loadings from Cootes were assumed to be reduced by 17% (34 kg TP/day) at the final HH RAP scenario. Notably, because of the greater uncertainty associated with the Cootes loadings, the probability distributions assigned were relatively flatter than those used to characterize other sources (Table S1). The average TP loadings from Redhill and Grindstone Creeks varied from 22.2 and 15 kg TP/day to 18.5 and 12.5 kg TP/day, respectively. It should also be noted that the latter loading values account for the contribution of the urban runoff, as quantified in the HHTT-CLR (2004) report. Following the calculations of the latter study, we also assumed an average loading of 52.7 kg TP/day and 135.4 kg NH_3/day (present conditions) from the combined sewer overflows, which was reduced by 91% (5 kg TP/day) and 85% (20 kg NH_3/day) at the final scenario.

Under the present loading conditions, the average TP and chlorophyll *a* concentrations were 28.06 ± 2.92 μg/L and 16.77 ± 0.97 μg chlα/L during the summer stratified period, while the predicted distributions were lying well above the existing water quality criteria of 17 μg TP/L and 10 μg chlα/L (Fig. 8a,b). The reduction of the total TP loading by

Table 2
Analysis of Scenarios: Exogenous loadings scenarios and corresponding flows in the Hamilton Harbour.

	Source	Flow (m^3/sec)	TP (kg/day)	PO_4 (kg/day)	TN (kg/day)	NO_3 (kg/day)	NH_3 (kg/day)
Present condition	Redhill and Urban Runoff	0.666	22.2	4.4	225.1	165.6	17.0
	Grindstone and Urban Runoff	0.767	15.0	3.0	370.8	272.8	28.0
	Combined Sewer Overflows	0.290	52.7	10.5	670.8	402.5	135.4
	Steels Mills	0	6.0	1.2	134.8	74.3	60.5
	Woodward	3.970	194.2	58.3	6102.3	2309.0	3023.6
	Skyway	1.248	20.4	6.1	420.1	119.8	155.9
	Cootes Paradise	2.777	40.8	10.2	443.9	120.0	12.0
	Total	9.719	351	94	8368	3464	3432
Scenario 1	Redhill and Urban Runoff	0.666	18.5	3.7	212.3	165.6	17
	Grindstone and Urban Runoff	0.767	12.5	2.5	349.8	272.8	28
	Combined Sewer Overflows	0.290	25	5	597.9	472.9	65
	Steels Mills	0	0	0	134.8	134.8	0
	Woodward	3.970	155	31	5792.6	3532.6	1800
	Skyway	1.248	15	3	338.3	160.7	115
	Cootes Paradise	2.777	34	6.8	356.3	132.0	6
	Total	9.719	260	52	7782	4871	2031
Scenario 2	Redhill and Urban Runoff	0.666	18.5	3.7	212.3	165.6	17
	Grindstone and Urban Runoff	0.767	12.5	2.5	349.8	272.8	28
	Combined Sewer Overflows	0.290	25	5	597.9	472.9	65
	Steels Mills	0	0	0	134.8	134.8	0
	Woodward	3.970	120	24	5562.6	4432.6	900
	Skyway	1.248	15	3	338.3	160.7	115
	Cootes Paradise	2.777	34	6.8	356.3	132.0	6
	Total	9.719	225	45	7552	5771	1131
RAP Proposition	Redhill and Urban Runoff	0.666	18.5	3.7	212.3	165.6	17
	Grindstone and Urban Runoff	0.767	12.5	2.5	349.8	272.8	28
	Combined Sewer Overflows	0.290	5	1	546.5	517.9	20
	Steels Mills	0	0	0	134.8	134.8	0
	Woodward	3.970	60	12	5438.1	4802.6	530
	Skyway	1.248	12	2.4	338.3	160.7	115
	Cootes Paradise	2.777	34	6.8	356.3	132.0	6
	Total	9.719	142	28	7376	6186	716

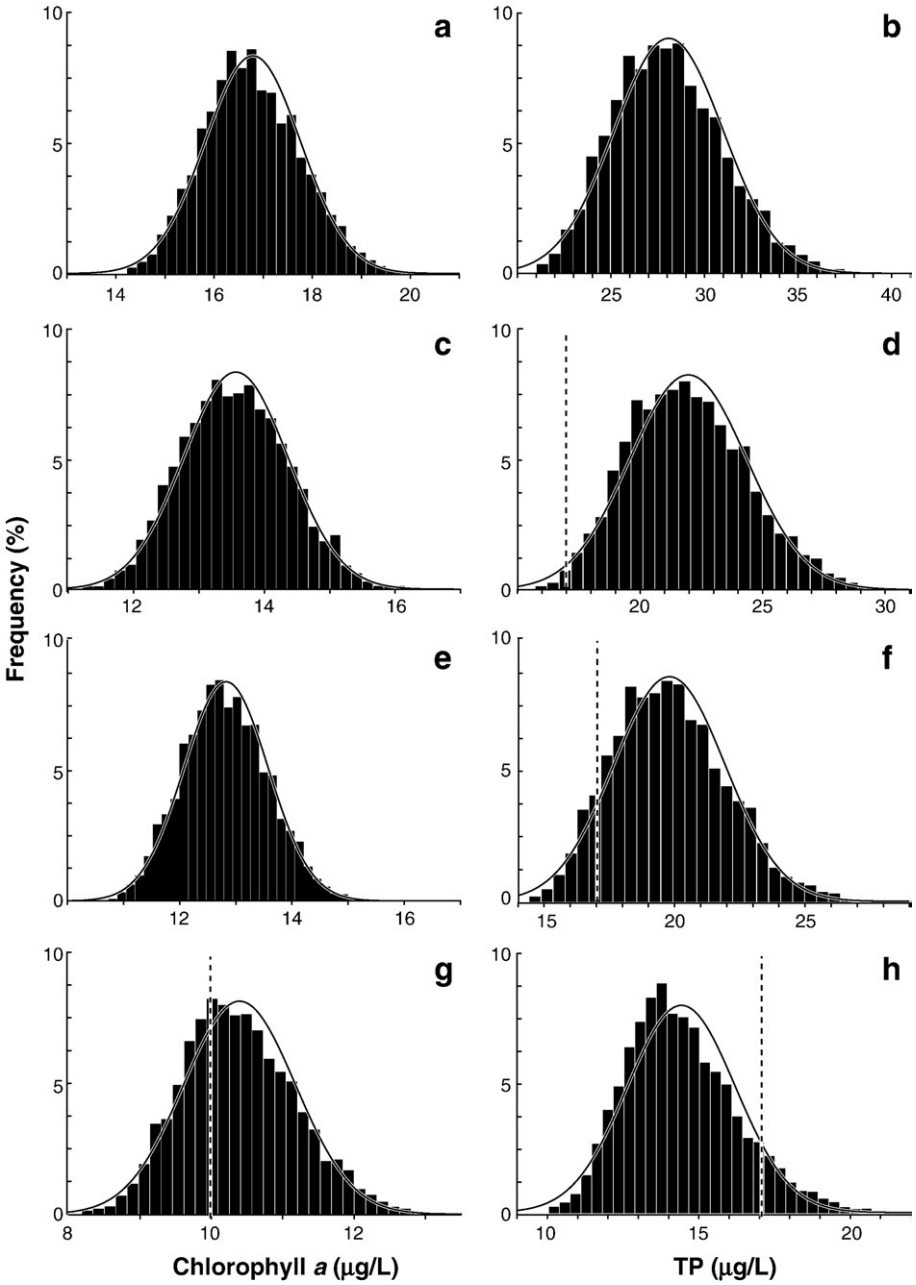

Fig. 8. Analysis of scenarios: exceedance frequency plots of chlorophyll a (a, c, e, g) and total phosphorus (b, d, f, h) concentrations for the present loading conditions (a, b), loading scenario No 1 (c, d), loading scenario No 2 (e, f) and the Hamilton Harbour RAP recommendations (g, h). Vertical dotted lines correspond to the 10-µg chl α/L and 17 µg TP/L water quality standards.

approximately 25% (260 ± 40 kg/day) does substantially improve the water quality conditions but does not result in an attainment of the targeted goals. That is, the average summer TP and chlorophyll *a* concentrations were 21.91 ± 2.39 µg/L and 13.54 ± 0. 79 µg chlα/L (Fig. 8c,d). Likewise, an additional reduction to the level of 225 ± 35 kg TP/day will primarily decrease the summer TP concentration (19.76 ± 2.14 µg/L) and secondarily the chlorophyll *a* levels (12.81 ± 0. 75 µg chlα/L), although the system will still not comply with the water quality standards (Fig. 8e, f). The implementation of the HH RAP loading propositions suggests that the projected average summer TP concentrations (14.39 ± 1.78 µg/L) will fall below the 17-µg TP/L threshold value, while the corresponding exceedance frequency will be about 7.5% (Fig. 8h). The average chlorophyll *a* concentration is predicted to be 10.39 ± 0.78 µg/L with >50% probability of exceeding the 10-µg chlα/L level (Fig. 8g).

Based on our model predictions, the summer epilimnetic algal growth is primarily limited by the light availability ($\varphi light_i < 0.2$) under the present loading conditions, whereas the role of phosphorus varies among the three functional groups depending on the phosphorus kinetics assigned ($\varphi PO4_{PFG\ A} > \varphi PO4_{PFG\ B} > \varphi PO4_{PFG\ C} > 0.25$). The implementation of the nutrient loading reduction schemes gradually shifts the system into a state of phosphorus limitation, which becomes the single most important limiting factor ($\varphi PO4_i \approx 0.15$–$0.20$) when the model is forced with the HH RAP nutrient loadings. However, because of the multiplicative formula used to postulate co-limiting effects of ambient light and nutrients on phytoplankton growth, our model also predicts that the accentuation of the phosphorus limitation will be partly counterbalanced by the improvement in the water clarity and thus the alleviation of the light limitation ($\varphi light_i \approx 0.30$–$0.35$). This finding contradicts Harris' (1980) results who found that the algae

are not self-shaded and therefore their growth is primarily limited by the high suspended matter in the Harbour. The gradual shifts of the prevailing conditions in the Harbour epilimnion are also reflected on the Chlα–TP relationships predicted for the different loading scenarios (Fig. 9a and Table 3). The slopes of the reported equations support the previous assertions of a stronger association between the two water quality variables induced by the nutrient loading reductions examined. In fact, the relationship presented for the HH RAP scenario ($Chl\alpha = 0.428 \times TP + 4.239$; $r^2 = 0.954$) was very similar to the one derived from a sub-sample of Monte Carlo runs with chlorophyll *a* to particulate phosphorus ratios>0.8 ($Chl\alpha = 0.438 \times TP + 4.084$; $r^2 = 0.937$). The latter value was used by Hiriart-Baer et al. (2009) to characterize *P* sufficient and *P* limited samples, and our analysis suggests that an average TP loading of 142 kg/day will establish a strongly phosphorus-limiting environment (>90% of the model runs sampled).

The relationships between the chlorophyll α and total phosphorus summer averages in the Harbour and the TP loadings from the different sources primarily highlight the critical role of the Woodward WWTP discharges (Fig. 10). In particular, the corresponding linear regression models explained about 65% of the overall chlorophyll α ($Chl\alpha_{Harbour} = 0.193 \times TP_{Woodward} + 13.071$; $r^2 = 0.656$) and total phosphorus ($TP_{Harbour} = 0.058 \times TP_{Woodward} + 16.899$; $r^2 = 0.659$) variability generated by the model. The second most important exogenous source was the Cootes Paradise accounting for 15% and 23% of the ambient Chlα and TP variability in the Harbour. We also note the relatively small proportion of the variability associated with the effluent loads from the Skyway WWTP (<2%), although existing evidence from the actual system suggests that the degradation in its performance can significantly impact the water quality (Charlton, 1997). The relationship of the epilimnetic summer TP with the total TP loading to the Harbour is also characterized by a plausible increase in the slope between the present conditions ($TP_{Harbour} = 0.058 \times TP_{Loading} + 7.866$) and the HH RAP scenario ($TP_{Harbour} = 0.067 \times TP_{Loading} + 5.193$), which suggests a tighter coupling between the ambient Harbour conditions and the exogenous nutrient loadings. Interestingly, the $TP_{Harbour}$ predictions of our linear regression equations are lower than those supported by the iron-modified Janus–Vollenweider relationship, e.g., instead of 23 μg/L, our analysis predicts approximately 20 μg/L at a critical loading level of 200 kg/day. Although both approaches account for iron-driven phosphorus precipitation to the bottom sediments, they do not share the same application domain for two basic reasons: (i) our equations refer to the summer TP average instead of the annual TP levels, and (ii) all the earlier empirical $TP_{Harbour}$-$TP_{Loading}$ relationships were framed upon a systematic error due to an underestimation of the loadings from the Woodward WWTP up to the year 2000 (Tanya Labencki, personal communication). Although a statistically robust correction to the existing empirical models has not been applied yet, we believe that this step is necessary for an objective intercomparison of the different water quality model predictions in the Harbour. Finally, in contrast with the Chapra and Dobson (1981) model, the $Chl\alpha_{Harbour}$–$TP_{Loading}$ regression equations derived from our Monte Carlo analysis (present conditions: $Chl\alpha_{Harbour} = 0.018 \times TP_{Loading} + 10.543$; HH RAP: $Chl\alpha_{Harbour} = 0.029 \times TP_{Loading} + 6.483$) support predictions of lower summer chlorophyll *a* concentrations and therefore appear to correct the systematic bias found during the application of the latter model in Hamilton Harbour.

Table 3
Relationships between the summer chlorophyll α and total phosphorus mean values in the Hamilton Harbour epilimnion for different nutrient loading conditions and zooplanktivory levels.

Nutrient loading	Zooplanktivory	
	Present	Change ($mz_j - 25\%$)
Present conditions	$Chl\alpha = 0.341 \times TP + 7.959$ ($r^2 = 0.895$)	$Chl\alpha = 0.244 \times TP + 5.810$ ($r^2 = 0.919$)
Scenario 1	$Chl\alpha = 0.317 \times TP + 6.594$ ($r^2 = 0.907$)	$Chl\alpha = 0.234 \times TP + 5.038$ ($r^2 = 0.938$)
Scenario 2	$Chl\alpha = 0.333 \times TP + 6.224$ ($r^2 = 0.906$)	$Chl\alpha = 0.234 \times TP + 5.090$ ($r^2 = 0.935$)
Hamilton Harbour RAP	$Chl\alpha = 0.428 \times TP + 4.239$ ($r^2 = 0.954$)	$Chl\alpha = 0.271 \times TP + 4.327$ ($r^2 = 0.963$)

The model considers an average hydraulic loading of 81.45×10^6 m^3 from fluvial and aerial sources during the summer stratified period. In the same time, the total (gross) inflows from Lake Ontario are 468.80×10^6 m^3 corresponding to an average inflow rate of 45 m^3/sec. After correcting for evaporative losses at the Harbour surface, these inputs represent an average residence time of 62 days during the stratified season, whereas the assumption that nearly all the Lake Ontario water (90%) enters the meso- and hypolimnion of the Harbour results in a hypolimnetic residence time of 31 days; both values are very close to those calculated by Hamblin and He (2003). The exogenous total phosphorus loadings contribute approximately 35.7×10^3 kg, while 9.9×10^3 kg of phosphorus flow out of the Harbour during the stratified season (Table S5). The total nitrogen, nitrate, and ammonia exogenous inputs supply 877, 360, and 372×10^3 kg into the system, while the losses through the ship canal are 756, 664, and 22×10^3 kg, respectively (Table S6). According to the model outputs, the net phytoplankton growth (uptake minus basal metabolism) utilizes 551×10^3 kg of nitrogen and 18.6×10^3 kg of phosphorus. Phosphorus mineralization contributes 1.69×10^3 kg, and if we associate these fluxes with the plankton basal metabolism excreted directly as phosphate (12.2×10^3), we can infer that a substantial proportion of the phytoplankton phosphorus

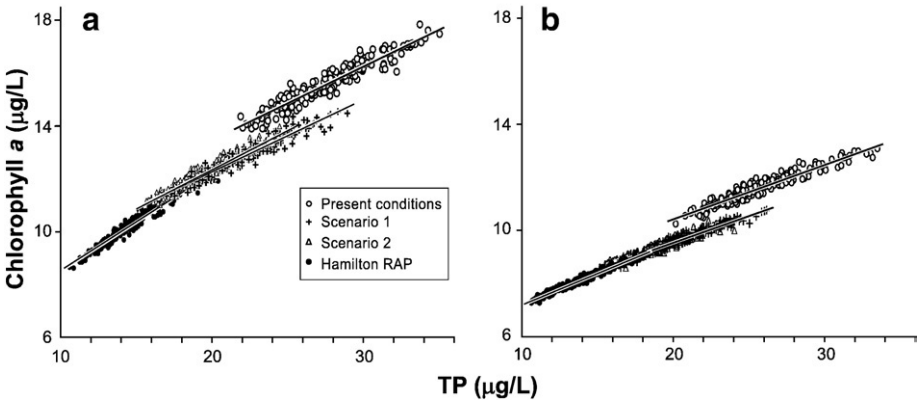

Fig. 9. Analysis of scenarios: relationships between chlorophyll α and total phosphorus in the Hamilton Harbour epilimnion based (a) on the current and (b) reduced by 25% zooplanktivory levels.

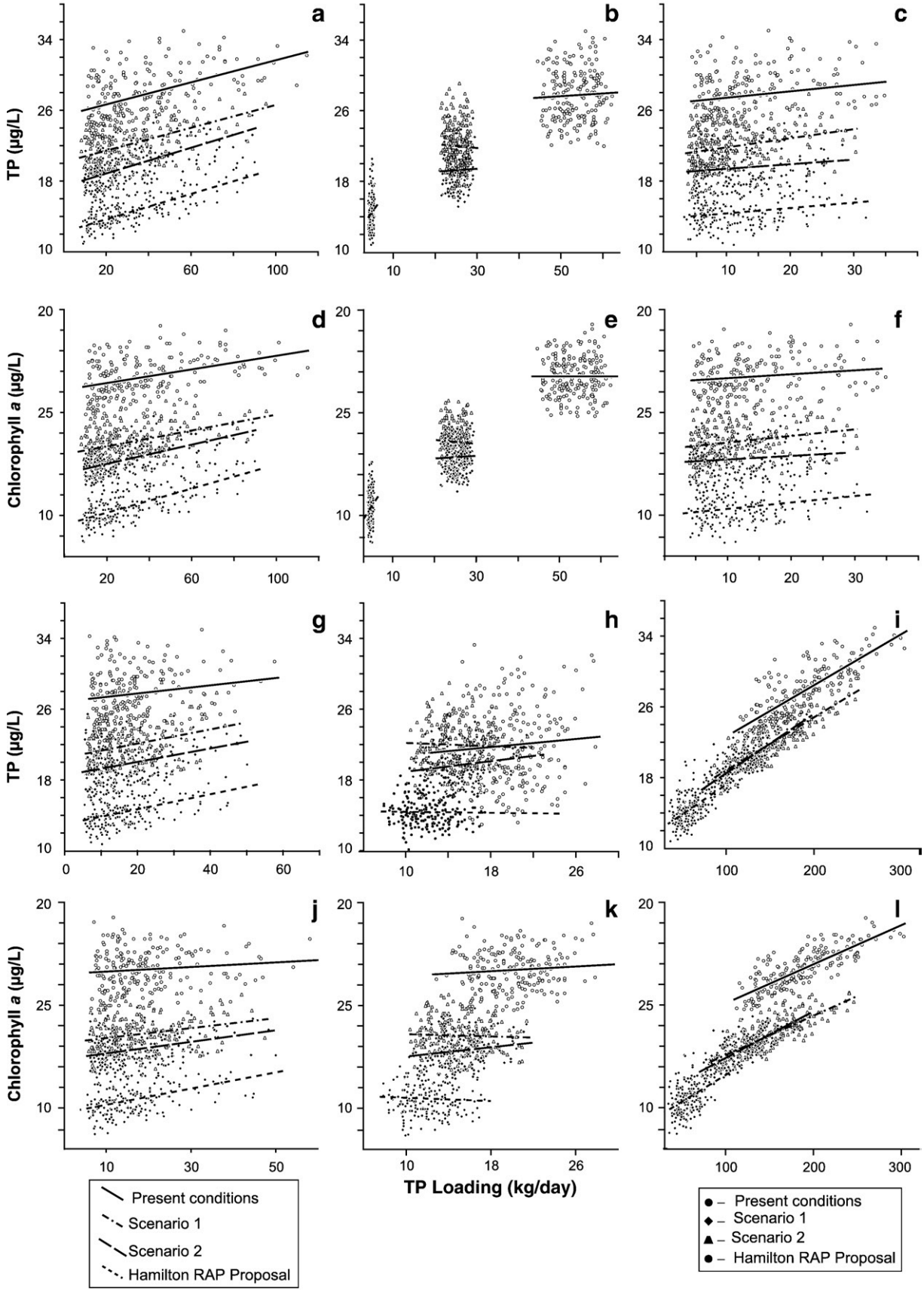

Fig. 10. Analysis of scenarios: relationships between chlorophyll α, total phosphorus, and the TP loadings from the different sources in the Hamilton Harbour area: Cootes Paradise (a, d); CSO (b, e); Grindstone Creek (c, f); Redhill Creek (g, j); Skyway WWTP (h, k); and Woodward WWTP (i, l).

demands in the mixed layer can be met by nutrient recycling. Phosphorus intrusion from the mesolimnion is estimated to be 4.4×10^3 kg, an estimate that comprises the diffusive exchanges as well as the Lake Ontario water masses entering the deeper part of the Harbour, displacing an equal volume of hypolimnetic water to the epilimnion. The model also provides evidence of particulate nitrogen and phosphorus downward fluxes of 543 and 48.3×10^3 kg, which is predicted to be reduced by approximately 50% under the HH RAP loading scenario. These values correspond to average sedimentation rates of 90 mg N/m^2/day and 11 mg P/m^2/day during the summer stratification, and the comparison of the latter estimates with the observed fluxes from the system will be critical to structurally validate the current model parameterization.

The role of zooplankton community

Thus far, our analysis suggests that the epilimnetic TP concentrations will decrease in response to the reduction of the external nutrient loadings and that the water quality standard of 17 μg TP/L will likely be met if the Hamilton Harbour RAP proposition for phosphorus loading at the level of 142 kg/day is achieved. The attainment of the water quality goal related to the summer chlorophyll *a* concentrations (5–10 μg/L) though has not been unequivocally demonstrated, as the central tendency of our projections indicates a marginal exceedance of the 10-μg/L threshold level, even when the exogenous loading conforms to the most extreme reduction guidelines. Among the existing Chl*α*–TP relationships in the recent local literature, the equations presented in Table 3 are relative close to the trajectory delineated by Hiriart-Baer et al. (2009) when using the data classified as *P* limited (see their Fig. 6). Our results differ from the relationship presented by the Burley (2007) study, which suggested that the summer chlorophyll *a* averages will be lower than 10 μg/L, once the summer TP levels fall below the 20-μg/L level (Fig. 11; p. 39 in Burley, 2007). The patterns implied by this graph, however, should be interpreted with caution if we consider that the form of this line (slope and intercept) is determined by three potentially influential points (i.e., high leverage values) corresponding to seasonal means from the Bay of Quinte and not from the Hamilton Harbour. Hence, given the lack of reliable information to assess the plausibility of our projections, the role of other potentially important factors in shaping the phytoplankton response to the variability of the ambient TP levels needs to be invoked; the most important being the control exerted from the zooplankton community.

As previously noted, the present parameterization essentially postulates a zooplankton community with two groups that mainly compete for the same food sources rather than having a prey (herbivores)–predator (carnivores) relationship. Given the absence of a distinct third trophic level from the model, the zooplankton mortality terms ($mz_{jj=\mathrm{herb,omni}}$) effectively act as surrogate parameters for the control exerted from carnivorous zooplankton and/or planktivorous fish. Thus, the importance of the top–down control is illustrated herein with a 25% reduction of zooplanktivory relative to the present levels (Table 3 and Fig. 9b). Indeed, our results show that the zooplankton abundance can significantly decrease the standing phytoplankton biomass in the system, thereby modulating the restoration rate as well as the stability of the new trophic state in the Harbour. The present model allocates approximately 15% of the total omnivorous/herbivorous zooplankton biomass to support the upper trophic levels, and it is noteworthy that a very similar range (14–17%) is being supported from an independent calibration exercise of a different food web structure (Ramin et al., submitted manuscript). If we consider all the sources of uncertainty associated with our calibration dataset though (e.g., assumptions made about what should be considered as "average" or reference conditions in the Harbour, errors stemming from the conversions from wet weight biomass to units of carbon, etc.), the question arising is: to what extent is the zooplankton parameterization presented herein, the optimal configuration to effectively depict the transition of the Harbour from a eutrophic to a mesotrophic state?

Gerlofsma et al. (2007) highlighted the relatively high chlorophyll *a*/total phosphorus ratios (0.41 to 0.62) in the Harbour which were interpreted as indicators of an odd-link system characterized by strong predation of zooplankton by fish (Mazumder, 1994). Evidence in support of the latter assertion was also provided by the smaller mean length of cladocerans (320–425 μm) in the Harbour relative to the Bay of Quinte (see their Fig. 7; p. 88), as fish preferentially consume larger zooplankton individuals and the mean zooplankton community length can reflect the balance between piscivores and planktivores within the fish community (Mills et al., 1987). In complete alignment with our results, Gerlofsma et al. (2007) argued that the level of planktivory should be a focal point of the restoration efforts and may shape the response rate of the system to the nutrient loading reductions, since the larger zooplankton taxa are particularly efficient in suppressing the standing phytoplankton biomass. Given that the Harbour is a nursery area for many young fish and that the high planktivory levels should be the norm, Gerlofsma et al. (2007) pinpointed the role of food web models to determine the optimum zooplankton composition and cladoceran size. In this regard, a follow-up study by Ramin et al. (submitted manuscript) examines different zooplankton configurations and discusses the broader implications for the Hamilton Harbour phytoplankton dynamics. Finally, another important regulatory factor could have been the abundance of the invasive zebra and quagga mussels, which is somewhat downplayed by the present model parameterization. Aside from the nearshore zones, Hamilton Harbour is one of the few shallow Great Lakes systems where dreissenids are not abundant, and the unsuitable, soft bottomed habitat beyond 8 m has limited the average biomass to about 1/10 of the densities experienced in Lake Erie and the Bay of Quinte (Dermott and Bonnell, 2007).

We also emphasize one more outstanding issue that should be pivotal in projecting the response of the planktonic communities to the expected changes of the ambient nutrient levels. Munawar and Fitzpatrick (2007) underscored the need to improve our understanding of the factors that drive the energy transfer within the microbial and planktonic food web. The same study argued that the high proportion of secondary to primary producers observed in Hamilton Harbour suggests that the autochthonous production may not likely be sufficient to sustain the food web. As a result, Munawar and Fitzpatrick (2007) hypothesized that other sources of autochthonous (benthic algae and macrophytes) and allochthonous energy may be equally important. The quantification of the relative support of consumers by autochthonous and allochthonous resources has received considerable attention, and several recent studies have shown that the impact of terrestrial subsidies depends on characteristics of the exogenous material, the pathway of entry into the food web, the zooplankton community structure, and the system productivity (Carpenter et al., 2005; Cole et al., 2006; Pace et al., 2007). Generally, allochthony seems to be low in both eutrophic lakes and oligotrophic, clear-water lakes, whereas the terrestrial subsidy to consumers is considered significant in relatively small systems with greater humic content, i.e., higher color and DOC (Pace et al., 2007). In our model, because of the absence of reliable estimates of exogenous particulate carbon loadings, we did not explicitly consider the carbon cycle and therefore the zooplankton depends exclusively on endogenous sources. While recent studies render support to our approach downplaying the role of allochthony (Brett et al., 2009), this feature of the model should be revisited in future refinements as it may unrealistically strengthen the coupling of the phytoplankton-zooplankton relationship in the Harbour.

Future improvements of the Hamilton Harbour model-Conclusions

We presented the results of a calibration exercise of an aquatic biogeochemical model and evaluated its ability to adequately reproduce

the average observed conditions along with the basic cause–effect relationships underlying the eutrophication problem in Hamilton Harbour. The model provides a good representation of several key water quality variables (chlorophyll *a*, total zooplankton biomass, phosphate, and total phosphorus) in the system, whereas significant discrepancies were identified with regards to the nitrate and ammonia levels and/or temporal variability. The zooplankton parameterization presented herein places more emphasis on the abundance relative to the nominal preferences for the different food sources, and therefore the two zooplankton groups had a competitive instead of a prey-predator relationship. Thus, our analysis highlights the importance of critically evaluating the representation of zooplankton community in the model, as the anticipated structural shifts of the zooplankton community and the subsequent strength of the top–down control will likely determine the recovery rate of the Harbour. Finally, several issues were raised during model calibration and validation (e.g., model misfit, lack of nitrogen data, and uncertainty about the loading estimates) that will guide the refinement of the model and the future research in the Harbour.

Structural augmentations of the model

The Hamilton Harbour model in its present form does not explicitly simulate the processes leading to the ice formation and melting. The segment-specific water temperatures are externally imposed as forcing functions, whereas the background light attenuation coefficient combined with a piecewise approach was used to reproduce the illumination of the water column during the ice-covered period (Huber et al., 2008). We found that the *Kextb* value presented in Appendix A was the optimal for reproducing the relatively high phytoplankton biomass levels in the winter (≈5 μg chl*α*/L), while the ice-free *Kextb* value was purposely kept at the same value to account for the effects of other factors (unrelated to the algal self-shading effects) affecting the underwater light attenuation (e.g., suspended solids). However, given that earlier work emphasized the importance of the high suspended matter as the primary limiting factor in the Harbour (Harris, 1980), the incorporation of a simple mass balance of suspended solids along with the explicit consideration of their role in the light attenuation may be warranted.

Furthermore, the duration of the ice cover period can also be particularly important for the dynamics of lakes, as several recent studies indicated that reduced ice cover and increasing water temperatures can result in more intense and earlier spring blooms (Peeters et al., 2007; Huber et al., 2008). Surprisingly, there is lack of consistent information with regards to the timing and magnitude of the spring phytoplankton bloom in the Harbour (e.g., Fig. 3a in Hiriart-Baer et al., 2009). As previously mentioned, the sampling cruises typically start after the first or second week of May which may coincide with the recession rather than the peak of the spring (diatom-dominated) bloom in Hamilton Harbour. While this piece of information may not be directly related to the dynamics of the system during the summer stratified period, it does allow to more accurately quantifying the amount of biogenic material that deposits on the bottom of the system before the onset of stratification. This particulate pool can be easily decomposed during the summer and can potentially account for a significant proportion of the sediment oxygen demand. The current version of the model predicts that the spring bloom can easily exceed the level of 20 μg chl*α*/L. Although we believe that this is not an unrealistic prediction, given that the model accurately predicts the subsequent zooplankton peak, but still warrants confirmation against data obtained from the system during the third or fourth week of April, i.e., a period that is more likely to coincide with the initiation or the peak of the spring bloom.

One of the major assumptions usually made when estimating the nutrient loadings from Cootes Paradise is that the flows into the system equal the outflows into the Harbour. The validity of this practice has been questioned in that it may underestimate the discharges due to diffusive mixing driven by the water quality gradients and/or the lake seiches (HHTT-CLR, 2004). The Cootes Paradise is a highly productive system with high chl*α* (>30 μg/L) and TP (>50 μg/L) concentrations (Chow-Fraser et al., 1998). Our model does not explicitly consider the amount of phytoplankton biomass exported from Cootes, assuming that the impact to the offshore waters of Hamilton Harbour may be minimal (Hiriart-Baer et al., 2009). However, the substantial uncertainty associated with the corresponding loadings may justify the development of a process-based model for Cootes to gain mechanistic insights into interplay between the two systems.

Modeling hypolimnetic hypoxia

The HH RAP is reevaluating the DO-related targets to determine what DO standard is biologically meaningful and attainable, as the current scientific consensus is that the goal of Harbour water always above 4 mg DO/L is unrealistic (HHTT-WQ, 2007). The elucidation of the relative importance of the different mechanisms that drive the hypolimnetic depletion rates has been a controversial issue in the Hamilton Harbour. Earlier work by Snodgrass and Ng (1985) primarily emphasized the importance of nitrification and sediment oxygen demand, arguing that the control of inputs of allochthonous carbonaceous materials will not be the most effective remediation strategy. It was also pointed out that the most significant improvement to the hypolimnetic dissolved oxygen deficit will be brought by a reduction in the rate of ammonia input (to reduce the rate of nitrification), a reduction in the rate of phosphorus input (to reduce the formation of organics), and dredging of the sediment (to reduce sediment oxygen demand). The nitrogenous oxygen demand is also suggested to contribute on average 50% of the total oxygen demand in the hypolimnion (Hiriart-Baer et al., 2009). By contrast, Roy et al. (1996) found that the CH_4 metabolism in Hamilton Harbour sediment is more important than nitrification as a sink of hypolimnetic O_2 and that the CH_4 oxidation by methanotrophs most likely decreases nitrification through competition for O_2. The same study also hypothesized that the methanotrophic activity may short-circuit the nitrogen cycle through immobilization of NH_4^+ (Roy et al., 1996).

Similar to Kellershohn and Tsanis (1999) study, our model assigns a significant role to the nitrification, and the current calibration vector predicts nitrification levels of 5–15 mg/m^3/day in the water column and 8–20 mg/m^2/day in the sediment. Because we currently do not have empirical estimates on the nitrification rates in the Harbour, these values are critical to be validated. Generally, in regards to Hamilton Harbour hypoxia, we believe that any modeling efforts should not be viewed as a strict inverse solution exercise. For example, several of the simulated processes of the nitrogen biogeochemical cycle (i.e., nitrification, denitrification, bacterial mineralization, particulate nitrogen fluxes, sediment–water interactions) can be easily adjusted to obtain an excellent fit to the observed nitrogen levels. However, the same processes are also closely related to the manifestation of hypolimnetic hypoxia, and given the overparameterized framework at hand; it is extremely easy to get "good results for wrong reasons". Unless reliable information from the system becomes available to properly constrain and/or validate the associated rates, our intent is to adopt probabilistic analyses of scenarios framed upon sophisticated sediment diagenesis submodels (Di Toro, 2001; Dittrich et al., 2009). In this case, a more refined segmentation (e.g., 5–10 completely mixed boxes) may be more appropriate to accommodate the spatiotemporal patterns of the inflowing water from Lake Ontario, which appears to be particularly important in replenishing oxygen in the hypoxic areas of the Harbour during the summer stratified period (Coakley et al., 2002; Rao et al., 2009).

Modeling toxic cyanobacteria blooms

The Harbour experiences erratic outbreaks of noxious and toxin-producing cyanobacteria (*Microcystis*), despite the substantial

decrease of the TP levels in the system (Murphy et al., 2003; Watson et al., 2008). These patterns of cyanobacteria dominance may seem counterintuitive as the existing paradigm predicts that their capacity to outcompete the usual eukaryotic residents of the summer phytoplankton communities (e.g., chlorophytes) decreases under low phosphorus availability (Hyenstrand et al., 2001). Among the several theories proposed to explain such structural shifts (Soranno, 1997; Lathrop et al., 1998; Hyenstrand et al., 1998; Downing et al., 2001; Watson et al., 2008), recent research has examined the likelihood that cyanobacteria dominance is induced by the elevated iron levels in the system (Medeiros and Molot, 2006). Because of their higher cellular iron requirements, it was hypothesized that the loadings from exogenous (e.g., WWTPs, steel mills) and/or endogenous (anoxic sediments) sources may be partly responsible for the manifestation of cyanobacteria blooms in the system (Medeiros and Molot, 2006). Although the results are somewhat inconclusive with regards to the strength of the relationships between iron and cyanobacteria abundance in the meso-eutrophic waters of the Harbour, Medeiros and Molot (2006) advocated the use of biological removal methods rather than iron chloride flocculation in the WWTPs to control the ambient iron levels. Watson et al. (2008) emphasized the importance of a more "fine-grained" approach that will integrate aspects of all the single-factor hypotheses presented in the literature, such as the buoyancy regulation, ability to fix molecular nitrogen, N–P ratios, minimization of mortality through an immunity to grazing by zooplankton, ability to outcompete most other phytoplankton for ammonium nitrogen. In particular, regarding the latter factor, we found that the relative composition of the phytoplankton community predicted by the model is particularly sensitive to the values assigned to the strength of the ammonium inhibition for nitrate uptake (ψ). Greater ψ values coupled with elevated levels of phosphorus appear to promote the relative abundance of our PFG C group (cyanobacteria, dinoflagellates) during the summer stratified period. This finding may also render support to Hiriart-Baer et al.'s (2009) assertions that the Hamilton Harbour phytoplankton dynamics could at times be modulated by the nitrogen availability.

Bayesian calibration and uncertainty analysis

The probabilistic assessment of the Harbour water quality conditions presented in this study accounts for the interannual variability (or uncertainty) of the exogenous nutrient loading conditions but does not accommodate the parametric uncertainty as well as the model structural error. An efficient means to address this particular weakness of our analysis is the implementation of Bayesian inference techniques to calibrate the model (Arhonditsis et al., 2007). Model uncertainty analysis essentially aims to quantify the joint probability distribution of all the model inputs and to make inference about this distribution. In this regard, Bayes' Theorem provides a convenient way to combine any existing information about the model inputs (prior) with current observations from the system (likelihood) and probabilistically assess the anticipated ecosystem responses (posterior). Thus, the Bayesian approach is more informative than the conventional model calibration practices and can be used to refine our knowledge of model input parameters and to obtain predictions along with uncertainty bounds for modelled output variables (Arhonditsis et al., 2007, 2008a,b). The iterative nature of the proposed calibration scheme is also conceptually similar to the policy practice of adaptive management (or "learning while doing") and can be used to optimize the spatiotemporal sampling efficiency of the existing monitoring programs (see Fig. 8 in Zhang and Arhonditsis, 2008). We believe that both outcomes are highly relevant to the Harbour conservation practices. The substantial uncertainty associated with the present and future water quality conditions makes compelling the development of a long-term methodological framework that can continuously update and rigorously evaluate the success of the contemporary restoration efforts, thereby providing the basis for revised (and improved) management actions in the Harbour (Hall et al., 2006).

Acknowledgement

This project has received funding support from the Ontario Ministry of the Environment (Canada-Ontario Grant Agreement 120808). Such support does not indicate endorsement by the Ministry of the contents of this material. Alex Gudimov has also received support from a UTSC Research Fellowship (Master of Environmental Science Program, Centre for Environment & University of Toronto at Scarborough). We wish to thank Duncan Boyd and Tanya Labencki (Ontario Ministry of the Environment) for their insightful comments on an earlier version of the manuscript. All the material pertinent to this study is available upon request from the corresponding author.

Appendix A. Description and calibration values of model parameters

Symbol	Description	Values	Units	Sources
AH_{PFGA}	Half saturation constant for ammonium uptake by PFG A	100	mg N/m^3	10
AH_{PFGB}	Half saturation constant for ammonium uptake by PFG B	80	mg N/m^3	10
AH_{PFGC}	Half saturation constant for ammonium uptake by PFG C	60	mg N/m^3	10
$\alpha_{DOC\ herbi}$	Fraction of herbivorous zooplankton mortality becoming dissolved organic carbon	0.5	-	10
$\alpha_{DOC\ omni}$	Fraction of omnivorous zooplankton mortality becoming dissolved organic carbon	0.5	-	10
$\alpha_{DOC\ PFGA}$	Fraction of PFG A mortality becoming dissolved organic carbon	0.5	-	10
$\alpha_{DOC\ PFGB}$	Fraction of PFG B mortality becoming dissolved organic carbon	0.5	-	10
$\alpha_{DOC\ PFGC}$	Fraction of PFG C mortality becoming dissolved organic carbon	0.5	-	10
αNH_4	Sediment ammonium release rate	0.5	mg NH_4 /m^2 day	
$\alpha NH_{4\ herbi}$	Fraction of herbivorous zooplankton mortality becoming ammonium	0.5	-	10
$\alpha NH_{4\ omni}$	Fraction of omnivorous zooplankton mortality becoming ammonium	0.5	-	10
$\alpha NH_{4\ PFGA}$	Fraction of PFG A mortality becoming ammonium	0.5	-	10
$\alpha NH_{4\ PFGB}$	Fraction of PFG B mortality becoming ammonium	0.5	-	10
$\alpha NH_{4\ PFGC}$	Fraction of PFG C mortality becoming ammonium	0.5	-	10
α_{NO3}	Sediment nitrate release rate	0.5	mg NO_3 /m^2 day	
α_{PO4}	Sediment phosphate release rate	0.5	mg PO_4 /m^2 day	
$\alpha_{PO4\ herbi}$	Fraction of herbivorous zooplankton mortality becoming phosphate	0.8	-	10

Appendix A (*continued*)

Symbol	Description	Values	Units	Sources
$\alpha_{PO4\ omni}$	Fraction of omnivorous zooplankton mortality becoming phosphate	0.8	-	10
$\alpha_{PO4\ PFGA}$	Fraction of PFG A mortality becoming phosphate	0.8	-	10
$\alpha_{PO4\ PFGB}$	Fraction of PFG B mortality becoming phosphate	0.8	-	10
$\alpha_{PO4\ PFGC}$	Fraction of PFG C mortality becoming phosphate	0.8	-	10
$asfood_{herbi\ det}$	Herbivorous zooplankton assimilation efficiency for detritus	0.45	-	
$asfood_{herbi\ PFGA}$	Herbivorous zooplankton assimilation efficiency for PFG A	0.5	-	
$asfood_{herbi\ PFGB}$	Herbivorous zooplankton assimilation efficiency for PFG B	0.5	-	
$asfood_{herbi\ PFGC}$	Herbivorous zooplankton assimilation efficiency for PFG C	0.15	-	
$asfood_{omni\ det}$	Omnivorous zooplankton assimilation efficiency for detritus	0.45	-	
$asfood_{omni\ herb}$	Omnivorous zooplankton assimilation efficiency for herbivorous zooplankton	0.55	-	
$asfood_{omni\ PFGA}$	Omnivorous zooplankton assimilation efficiency for PFG A	0.5	-	
$asfood_{omni\ PFGB}$	Omnivorous zooplankton assimilation efficiency for PFG B	0.5	-	
$asfood_{omni\ PFGC}$	Omnivorous zooplankton assimilation efficiency for PFG C	0.15	-	
$Chl\alpha C_{PFGA}$	Chlorophyll to carbon ratio in PFG A	0.02	-	8,9,11,15
$Chl\alpha C_{PFGB}$	Chlorophyll to carbon ratio in PFG B	0.02	-	8,9,11,15
$Chl\alpha C_{PFGC}$	Chlorophyll to carbon ratio in PFG C	0.02	-	8,9,11,15
$Denitrifmax$	Maximum denitrification rate	5	mg N/m^3/day	
$Denitrifmax_{sed}$	Maximum sediment denitrification rate	25	mg N/m^2/day	
$Ffilter_{PFGA}$	PFG A filtering rate from dreissenids	0.02	1/day	
$Ffilter_{PFGB}$	PFG B filtering rate from dreissenids	0.015	1/day	
$Ffilter_{PFGC}$	PFG C filtering rate from dreissenids	0.01	1/day	
$gwthmax_{PFGA}$	Maximum growth for PFG A	2.3	1/day	13,14
$gwthmax_{PFGB}$	Maximum growth for PFG B	2	1/day	13,14
$gwthmax_{PFGC}$	Maximum growth for PFG C	1.7	1/day	13,14
$H_{epilimnion}$	Distance from water surface to top of the epilimnion segment layer	0	m	
$H_{metalimnion}$	Distance from water surface to top of the metalimnion segment	8	m	
$H_{hypolimnion}$	Distance from water surface to top of the hypolimnion segment	16	m	
Ik_{PFGA}	Half saturation light intensity for PFG A	150	MJ $/m^2$ day	
Ik_{PFGB}	Half saturation light intensity for PFG B	150	MJ $/m^2$ day	
Ik_{PFGC}	Half saturation light intensity for PFG C	150	MJ $/m^2$ day	
$KCrefmineral$	Particulate carbon mineralization rate at reference temperature	0.01	1/day	
$Kextb$	Background light attenuation	0.15	1/m	15
$Kextchla_{PFGA}$	Light attenuation coefficient for PFG A	0.04	m^2/mg	13,15
$Kextchla_{PFGB}$	Light attenuation coefficient for PFG B	0.04	m^2/mg	13,15
$Kextchla_{PFGC}$	Light attenuation coefficient for PFG C	0.05	m^2/mg	13,15
$KHdodenit$	Half saturation concentration of DO deficit required for nitrification	0.5	$mgO_2\ m^{-3}$	10
$KHdodenit_{sed}$	Half saturation concentration of DO deficit required for denitrification in the sediments	1	mg O_2 $/m^3$	
$KHdonit$	Half saturation concentration of DO required for nitrification	1	mg O_2 $/m^3$	10
$KHdonit_{sed}$	Half saturation concentration of DO required for nitrification in the sediments	2	mg O_2 $/m^3$	
$KHnh4nit$	Half saturation concentration of ammonium required for nitrification	1	mg N/m^3	10
$KHnh4nit_{sed}$	Half saturation concentration of ammonium required for nitrification in the sediments	75	mg N/m^3	
$KHno3denit$	Half saturation concentration of nitrate required for denitrification	15	mg N/m^3	10
$KHno3denit_{sed}$	Half saturation concentration of DO deficit required for denitrification in the sediments	15	mgO_2/m^3	
$KNrefmineral$	Nitrogen mineralization rate at reference temperature	0.01	1/day	10,15
$KPrefmineral$	Phosphorus mineralization rate at reference temperature	0.005	1/day	3,15,10
kt	Effects of temperature on phytoplankton mortality	0.069	$1/^oC$	3, 7,10,11
$ktfilt$	Effects of temperature on phytoplankton filtration	0.069	$1/^oC$	
$KTFmin$	Effects of temperature on mineralization	0.004	$1/^oC^2$	
$KTgrdenitr$	Effect of temperature on denitrification	0.004	$1/^oC^2$	
$KTgrdenitr_{sed}$	Effect of temperature on sediment denitrification	0.004	$1/^oC^2$	
$KTgr_{herbi}$	Effect of temperature on herbivorous zooplankton	0.005	$1/^oC^2$	1-2-3-4-5
$KTgrnitr$	Effect of temperature on nitrification	0.004	$1/^oC^2$	10,16
$KTgrnitr_{sed}$	Effect of temperature on sediment nitrification	0.004	$1/^oC^2$	
$KTgr_{omni}$	Effect of temperature on omnivorous zooplankton	0.005	$1/^oC^2$	2,3
$KTgr_{PFGA}$	Effect of temperature on PFG A	0.005	$1/^oC^2$	3,10,13,14
$KTgr_{PFGB}$	Effect of temperature on PFG A	0.005	$1/^oC^2$	3,10,13,14
$KTgr_{PFGB}$	Effect of temperature on PFG B	0.005	$1/^oC^2$	3,10,13,14
$KTgr_{PFGC}$	Effect of temperature on PFG C	0.005	$1/^oC^2$	3,10,13,14
kt_{sed}	Effects of temperature on sedimentation	0.004	-	
KZ_{herbi}	Half saturation constant for grazing by herbivorous zooplankton	105	mg C $/m^3$	6-7
KZ_{omni}	Half saturation constant for grazing by omnivorous zooplankton	105	mg C $/m^3$	6,7
$maxgrazing_{herbi}$	Maximum grazing rate for herbivorous zooplankton	0.5	1/day	6-7
$maxgrazing_{omni}$	Maximum grazing rate for omnivorous zooplankton	0.5	1/day	6,9
mp_{PFGA}	Mortality rate for PFG A	0.045	1/day	3,7,10,11,15
mp_{PFGB}	Mortality rate for PFG B	0.025	1/day	3,7,10,11,15
mp_{PFGC}	Mortality rate for PFG C	0.015	1/day	3,7,10,11
mz_{herbi}	Mortality rate for herbivorous zooplankton	0.15	1/day	1,3, 6,7, 8,9
mz_{omni}	Mortality rate for omnivorous zooplankton	0.17	1/day	1-3, 6,7,9
NC_{herbi}	Nitrogen to carbon ratio for omnivorous zooplankton	0.2	mg N/ mg C	17,18
NC_{omni}	Nitrogen to carbon ratio for herbivorous zooplankton	0.2	mg N/ mg C	17,18
NH_{PFGA}	Half saturation constant for nitrate uptake by PFG A	100	mg N/m^3	13-15
NH_{PFGB}	Half saturation constant for nitrate uptake by PFG B	80	mg N/m^3	13-15
NH_{PFGC}	Half saturation constant for nitrate uptake by PFG C	60	mg N/m^3	13-15
$Nitrifmax$	Maximum nitrification rate at optimal temperature	20	mg N/m^3day	10,15,16
$Nitrifmax_{sed}$	Maximum sediment nitrification rate	50	mg N $/m^2$day	
PC_{herbi}	Phosphorus to carbon ratio for herbivorous zooplankton	0.025	mg P/ mg C	17,18

(*continued on next page*)

Appendix A (*continued*)

Symbol	Description	Values	Units	Sources
PC_{omni}	Phosphorus to carbon ratio for omnivorous zooplankton	0.025	mg P/mg C	17,18
PH_{PFGA}	Half saturation constant for phosphorus uptake by PFG A	10	mg P/ m^3	9,13,14
PH_{PFGB}	Half saturation constant for phosphorus uptake by PFG B	12	mg P/ m^3	9,13,14
PH_{PFGC}	Half saturation constant for phosphorus uptake by PFG C	20	mg P/ m^3	9,13,14
$Pmax_{PFGA}$	Maximum PFG A internal phosphate	0.025	mg P /mg C	7,13,15
$Pmax_{PFGB}$	Maximum PFG B internal phosphate	0.025	mg P/ mg C	7,13,15
$Pmax_{PFGC}$	Maximum PFG C internal phosphate	0.025	mg P/ mg C	7,13,15
$Pmaxuptake_{PFGA}$	Maximum phosphorus uptake rate for PFG A	0.02	mg P/ mg C day	7,13,15
$Pmaxuptake_{PFGB}$	Maximum phosphorus uptake rate for PFG B	0.015	mg P/ mg C day	7,13,15
$Pmaxuptake_{PFGC}$	Maximum phosphorus uptake rate for PFG C	0.01	mg P/ mg C day	7,13,15
$Pmin_{PFGA}$	Minimum PFG A internal phosphorus	0.008	mg P/ mg C	7,13,15
$Pmin_{PFGB}$	Minimum PFG B internal phosphorus	0.008	mg P/ mg C	7,13,15
$Pmin_{PFGC}$	Minimum PFG C internal phosphorus	0.008	mg P/ mg C	7,13,15
$Pref_{herbi\ det}$	Preference of herbivorous zooplankton for detritus	1	-	
$Pref_{herbi\ PFGA}$	Preference of herbivorous zooplankton for PFG A	1.5	-	
$Pref_{herbi\ PFGB}$	Preference of herbivorous zooplankton for PFG B	1	-	
$Pref_{herbi\ PFGC}$	Preference of herbivorous zooplankton for PFG C	0.5	-	
$Pref_{omnidet}$	Preference of omnivorous zooplankton for detritus	1	-	
$Pref_{omniherbi}$	Preference of omnivorous zooplankton for herbivorous zooplankton	1.5	-	
$Pref_{omniPFGA}$	Preference of omnivorous zooplankton for PFG A	1	-	
$Pref_{omniPFGB}$	Preference of omnivorous zooplankton for PFG B	1	-	
$Pref_{omniPFGC}$	Preference of omnivorous zooplankton for PFG C	0.5	-	
$Tempref$	Water reference temperature	20	°C	3,7,10,11
$Tempref_{sed}$	Sediment reference temperature	20	°C	
$Toptdenitr$	Optimal temperature for denitrification	20	°C	
$Toptdenitr_{sed}$	Optimal temperature for denitrification in sediment	20	°C	
$Topt_{herbi}$	Reference temperature for herbivorous zooplankton	20	°C	1-5
$Toptmin$	Optimal temperature for mineralization	20	°C	
$Toptnitr$	Optimal temperature for nitrification	20	°C	10,16
$Toptnitr_{sed}$	Optimal temperature for denitrification in sediment	20	°C	
$Topt_{omni}$	Reference temperature for omnivorous zooplankton	20	°C	1-5
$Topt_{PFGA}$	Reference temperature for PFG A metabolism	20	°C	3,7,10,11
$Topt_{PFGB}$	Reference temperature for PFG B metabolism	22	°C	3,7,10,11
$Topt_{PFGC}$	Reference temperature for PFG C metabolism	24	°C	3,7,10,11
$Vset_{biogenic}$	Biogenic particle settling velocity	0.15	m/day	
$Vsettling$	Allochthonous particle settling velocity	0.65	m/day	8,10,13,14
$Vsettling_{PFGA}$	PFG A settling velocity	0.15	m/day	2,10-12
$Vsettling_{PFGB}$	PFG B settling velocity	0.1	m/day	2,10-12
$Vsettling_{PFGC}$	PFG C settling velocity	0.02	m/day	2,10-12
β_N	Fraction of inert nitrogen buried into deeper sediment	0.4	-	
β_P	Fraction of inert phosphorus buried into deeper sediment	0.9	-	
ψ	Strength of the ammonium inhibition for nitrate uptake	0.05	L/μg N	
$z_{epilimnion}$	depth of epilimnion department	8	m	
$z_{mesolimnion}$	depth of mesolimnion department	8	m	
$z_{hypolimnion}$	depth hypolimnion department	8	m	

1) Lampert and Sommer, 1997; 2) Wetzel, 2001; 3) Omlin et al., 2001; 4) Orcutt and Porter, 1983; 5) Downing and Rigler, 1984; 6) Sommer, 1989; 7) Jorgensen et al., 1991; 8) Wetzel, 2001; 9) Chen et al., 2002(and references therein); 10) Cerco and Cole, 1994(and references therein); 11) Reynolds, 1984; 12) Sandgren, 1991; 13) Arhonditsis and Brett, 2005a; 14) Reynolds, 2006; 15) Hamilton and Schladow, 1997 (and references therein); 16) Berounsky and Nixon, 1990; 17) Hessen and Lyche, 1991; 18) Sterner et al., 1992.

Appendix B. Supplementary data

Supplementary data associated with this article can be found, in the online version, at doi:10.1016/j.jglr.2010.04.001.

References

Ahlgren, I., Frisk, T., Kamp-Nielsen, L., 1988. Empirical and theoretical-models of phosphorus loading, retention and concentration vs lake trophic state. Hydrobiologia 170, 285–304.

Arhonditsis, G.B., Brett, M.T., 2005a. Eutrophication model for Lake Washington (USA). Part I. Model description and sensitivity analysis. Ecol. Model. 187, 140–178.

Arhonditsis, G.B., Brett, M.T., 2005b. Eutrophication model for Lake Washington (USA). Part II. Model calibration and system dynamics analysis. Ecol. Model. 187, 179–200.

Arhonditsis, G.B., Tsirtsis, G., Karydis, M., 2002. The effects of episodic rainfall events to the dynamics of coastal marine ecosystems: applications to a semi-enclosed gulf in the Mediterranean Sea. J. Marine Syst. 35, 183–205.

Arhonditsis, G.B., Qian, S.S., Stow, C.A., Lamon, E.C., Reckhow, K.H., 2007. Eutrophication risk assessment using Bayesian calibration of process-based models: application to a mesotrophic lake. Ecol. Model. 208 (2–4), 215–229.

Arhonditsis, G.B., Papantou, D., Zhang, W.T., Perhar, G., Massos, E., Shi, M.L., 2008a. Bayesian calibration of mechanistic aquatic biogeochemical models and benefits for environmental management. J. Mar. Syst. 73, 8–30.

Arhonditsis, G.B., Perhar, G., Zhang, W.T., Massos, E., Shi, M.L., Das, A., 2008b. Addressing equifinality and uncertainty in eutrophication models. Water Resour. Res. 44, W01420.

Barica, J., 1989. Unique limnological phenomena affecting water quality of Hamilton Harbour, Lake Ontario. J. Great Lakes Res. 15 (3), 519–530.

Berounsky, V.M., Nixon, S.W., 1990. Temperature and the annual cycle of nitrification in waters of Narragansett Bay. Limnol. Oceanogr. 35, 1610–1617.

Bierman, V.J., Kaur, J., DePinto, J.V., Feist, T.J., Dilks, D.W., 2005. Modeling the role of zebra mussels in the proliferation of blue-green algae in Saginaw Bay, Lake Huron. J. Great Lakes Res. 31 (1), 32–55.

Brett, M.T., Benjamin, M.M., 2008. A review and reassessment of lake phosphorus retention and the nutrient loading concept. Freshwater Biol. 53 (1), 194–211.

Brett, M.T., Muller-Navarra, D.C., Park, S.K., 2000. Empirical analysis of the effect of phosphorus limitation on algal food quality for freshwater zooplankton. Limnol. Oceanogr. 45 (7), 1564–1575.

Brett, M.T., Kainz, M.J., Taipale, S.J., Seshan, H., 2009. Phytoplankton, not allochthonous carbon, sustains herbivorous zooplankton production. P. Natl. Acad. Sci. USA 106, 21197–21201.

Burley, M., 2007. Water quality and phytoplankton photosynthesis. Can. Tech. Rep. Fish. Aquat. Sci. 2729, 9–42.

Carpenter, S.R., Cole, J.J., Pace, M.L., Van de Bogert, M., Bade, D.L., Bastviken, D., Gille, C.M., Hodgson, J.R., Kitchell, J.F., Kritzberg, E.S., 2005. Ecosystem subsidies: terrestrial support of aquatic food webs from C-13 addition to contrasting lakes. Ecology 86 (10), 2737–2750.

Cerco, C., Cole, T., 1993. 3-Dimensional Eutrophication Model of Chesapeake Bay. J. Environ. Eng.-ASCE 119, 1006–1025.

Chapra, S.C., Dobson, H.F.H., 1981. Quantification of the lake trophic typologies of Naumann (surface quality) and Thienemann (oxygen) with special reference to the Great Lakes. J. Great Lakes Res. 7 (2), 182–193.

Charlton, M.N. 1993. *Eutrophication Management in Hamilton Harbour: Hypolimnion Oxygen*. NWRI Contribution No. 93-02. January 13, 1993.

Charlton, M.N., 1997. The sewage issue in Hamilton Harbour: implications of population growth for the remedial action plan. Water Qual. Res. J. Can. 32 (2), 407–420.
Charlton, M.N., 2001. The Hamilton Harbour remedial action plan: eutrophication. Verh. Internat. Verein. Limnol. 27, 4069–4072.
Charlton, M.N., Le Sage, R., 1996. Water quality trends in Hamilton Harbour: 1987 to 1995. Water Qual. Res. J. Can. 31, 473–484.
Chen, C.S., Ji, R.B., Schwab, D.J., Beletsky, D., Fahnenstiel, G.L., Jiang, M.S., Johengen, T.H., Vanderploeg, H., Eadie, B., Budd, J.W., Bundy, M.H., Gardner, W., Cotner, J., Lavrentyev, P.J., 2002. A model study of the coupled biological and physical dynamics in Lake Michigan. Ecol. Model. 152, 145–168.
Chow-Fraser, P., Lougheed, V., Le Thiec, V., Crosbie, B., Simser, L., Lord, J., 1998. Long-term response of the biotic community to fluctuating water levels and changes in water quality in Cootes Paradise Marsh, a degraded coastal wetland of Lake Ontario. Wetl. Ecol. Manag. 6, 19–42.
Coakley, J.P., et al., 2002. Transport of sewage-contaminated sediment in northeastern Hamilton Harbour. J. Great Lakes Res. 28 (1), 77–90.
Cole, J.J., Carpenter, S.R., Pace, M.L., Van de Bogert, M.C., Kitchell, J.L., Hodgson, J.R., 2006. Differential support of lake food webs by three types of terrestrial organic carbon. Ecol. Lett. 9, 558–568.
Dermott, R., Bonnell, R., 2007. Benthic fauna in Hamilton Harbour: 2002-2003. Can. Tech. Rep. Fish. Aquat. Sci. 2729, 91–120.
Dermott, R., Johannsson, O., Munawar, M., Bonnell, R., Bowen, K., Burley, M., Fitzpatrick, M., Gerlofsma, J., Niblock, H., 2007. Assessment of lower food web in Hamilton Harbour, Lake Ontario, 2002–2004. Can. Tech. Rep. Fish. Aquat. Sci. 2729, 1–120.
Di Toro, D.M., 2001. Sediment Flux Modeling. J. Wiley and Sons, New York.
Dittrich, M., Wehrli, B., Reichert, P., 2009. Lake sediments during the transient eutrophication period: reactive-transport model and identifiability study. Ecol. Model. 220 (20), 2751–2769.
Downing, J.A., Rigler, F.H., 1984. A Manual on Methods for the Assessment of Second Productivity in Fresh Water, second ed. Blackwell Scientific Publications, Oxford, UK.
Downing, J.A., Watson, S.B., McCauley, E., 2001. Predicting Cyanobacteria dominance in lakes. Can. J. Fish. Aquat. Sci. 58, 1905–1908.
Edwards, A.M., Yool, A., 2000. The role of higher predation in plankton population models. J. Plankton Res. 22 (6), 1085–1112.
Environment Canada. 1981. *The OECD Cooperative Programme on Eutrophication*. Canadian Contribution. Compiled and prepared by L.L. Janus and R.A. Vollenweider. Scientific Series No. 131.
Eppley, R.W., Peterson, B.J., 1979. Particulate organic-matter flux and planktonic new production in the deep ocean. Nature 282 (5740), 677–680.
Fasham, M.J.R., Ducklow, H.W., McKelvie, S.M., 1990. A nitrogen-based model of plankton dynamics in the oceanic mixed layer. J. Mar. Res. 48, 591–639.
Gerlofsma, J., Bowen, K., Johannsson, O., 2007. Zooplankton in Hamilton Harbour 2002–2004. Can. Tech. Rep. Fish. Aquat. Sci. 2729, 65–90.
Hall, J.D., O'Connor, K., Ranieri, J., 2006. Progress toward delisting a great lakes area of concern: the role of integrated research and monitoring in the Hamilton Harbour remedial action plan. Environ. Monit. Assess. 113, 227–243.
Hamblin, P.F., He, C., 2003. Numerical models of the exchange flows between Hamilton Harbour and Lake Ontario. Can. J. Civ. Eng. 30, 168–180.
Hamilton Harbour RAP Technical Team (HH RAP). 2004. 1996–2002 Contaminant Loadings and Concentrations to Hamilton Harbour.
Hamilton Harbour Technical Team—Water Quality 2007. Hamilton Harbour RAP water quality goals and targets review, Part 1: Response to the City of Hamilton's proposed wastewater system upgrades, Technical appendix.
Hamilton, D.P., Schladow, S.G., 1997. Prediction of water quality in lakes and reservoirs. Part I—Model description. Ecol. Model. 96, 91–110.
Harris, G.P., 1980. Temporal and spatial scales in phytoplankton ecology, mechanics, methods, models and management. Can. J. Fish. Aquat. Sci. 37, 877–900.
Hessen, D.O., Lyche, A., 1991. Interspecific and intraspecific variations in zooplankton element composition. Arch. Hydrobiol. 121, 343–353.
Hiriart-Baer, V.P., Milne, J., Charlton, M.N., 2009. Water quality trends in Hamilton Harbour: two decades of change in nutrients and chlorophyll a. J. Great Lakes Res. 35 (2), 293–301.
Huber, V., Adrian, R., Gerten, D., 2008. Phytoplankton response to climate warming modified by trophic state. Limnol. Oceanogr. 53 (1), 1–13.
Hyenstrand, P., Blomqvist, P., Petersson, A., 1998. Factors determining cyanobacterial success in aquatic systems—a literature review. Arch. Hydrobiol. 51, 41–62.
Hyenstrand, P., Rydin, E., Gunnerhed, M., Linder, J., Blomqvist, P., 2001. Response of the cyanobacterium *Gloeotrichia echinulata* to iron and boron additions—an experiment from Lake Erken. Freshwater Biol. 46 (6), 735–741.
Janus, L.L. 1987. *Chlorophyll-nutrient relationships in Hamilton Harbour*. Memorandum from L.L. Janus, Science Liaison Division, to Dr. G.K. Rodgers, National Water Research Institute.
Jassby, A.D., Platt, T., 1976. Mathematical formulation of the relationship between photosynthesis and light for phytoplankton. Limnol. Oceanogr. 21, 540–547.
Jorgensen, S.E., Nielsen, S.N., Jorgensen, L.A., 1991. Handbook of ecological parameters and ecotoxicology. Pergamon Press, Amsterdam.
Kellershohn, D.A., Tsanis, I.K., 1999. 3D eutrophication modeling of Hamilton Harbour: analysis of remedial options. J. Great Lakes Res. 25 (1), 3–25.
Klapwijk, A., Snodgrass, W.J., 1985. Model for lake–bay exchange flow. J. Great Lakes Res. 11 (1), 43–52.
Lampert, W., Sommer, U., 1997. Limnoecology: The Ecology of Lakes and Streams. Oxford University Press.
Lathrop, R.C., Carpenter, S.R., Stow, C.A., Soranno, P.A., Panuska, J.C., 1998. Phosphorus loading reductions needed to control blue-green algal blooms in Lake Mendota. Source Can. J. Fish. Aquat. Sci. 55 (5), 1169–1178.
Mayer, T., Manning, P.G., 1990. Inorganic contaminants in suspended-solids from Hamilton Harbor. J. Great Lakes Res. 16 (2), 299–318.
Mazumder, A., 1994. Patterns of algal biomass in dominant odd-link vs even-link lake ecosystems. Ecology 75 (4), 1141–1149.
McMahon, J.A., and Snodgrass W.J. 1993. *Hamilton Harbour eutrophication modelling study*. Submitted to the Ontario Ministry of the Environment.
Medeiros, A.S., Molot, L.A., 2006. Trends in iron and phosphorus loading to Lake Ontario from waste water treatment plants in Hamilton and Toronto. J. Great Lakes Res. 32 (4), 788–797.
Mills, E.L., Green, D.M., Schiavone Jr., A., 1987. Use of zooplankton size to assess the community structure of fish populations in freshwater lakes. N. Am. J. Fish Manage. 7 (3), 369–378.
Molot, L.A., Dillon, P.J., Clark, B.J., Neary, B.P., 1992. Predicting end-of-summer oxygen profiles in stratified lakes. Can. J. Fish. Aquat. Sci. 49, 2263–2372.
Munawar, M., Fitzpatrick, M., 2007. An integrated assessment of the microbial and planktonic communities of Hamilton Harbour. Can. Tech. Rep. Fish. Aquat. Sci. 2729, 43–63.
Murphy, T.P., Irvine, K., Guo, J., Davies, J., Murkin, H., Charlton, M., Watson, S.B., 2003. New microcystin concerns in the lower great lakes. Water Qual. Res. J. Can. 38 (1), 127–140.
Omlin, M., Brun, R., Reichert, P., 2001. Biogeochemical model of Lake Zurich: sensitivity, identifiability and uncertainty analysis. *Ecol.* Model. 141 (1–3), 105–123.
Ontario Ministry of Environment (MOE), 1985. Hamilton Harbour Technical Summary and General Management Options.
Orcutt, J.D., Porter, K.G., 1983. Diel vertical migration by zooplankton—constant and fluctuating temperature effects on life-history parameters of daphnia. Limnol. Oceanogr. 28 (4), 720–730.
Pace, M.L., Carpenter, S.R., Cole, J.J., Coloso, J.J., Kitchell, J.F., Hodgson, J.R., Middelburg, J.J., Preston, N.D., Solomon, C.T., Weidel, B.C., 2007. Does terrestrial organic carbon subsidize the planktonic food web in a clear-water lake? *Limnol.* Oceanogr. 52, 2177–2189.
Peeters, F., Straile, D., Lorke, A., Ollinger, D., 2007. Turbulent mixing and phytoplankton spring bloom development in a deep lake. Limnol. Oceanogr. 52 (1), 286–298.
Rao, Yerubandi R., Marvin, C.H., Zhao, J., 2009. Application of a numerical model for circulation, temperature and pollutant distribution in Hamilton Harbour. J. Great Lakes Res. 35, 61–73.
Reynolds, C.S., 1984. The Ecology of Freshwater Phytoplankton. Cambridge University Press, Cambridge, UK.
Reynolds, C.S., 2006. The Ecology of Phytoplankton. Cambridge University Press.
Rodgers, G.K. 1998. *Winter stratification in Hamilton Harbour*. NWRI Contribution No. 98-231.
Roy, R., Knowles, R., Charlton, M.N., 1996. Nitrification and methane oxidation at the sediment surface in Hamilton Harbour (Lake Ontario). Can. J. Fish. Aquat. Sci. 53 (11), 2466–2472.
Rykiel Jr., E.J., 1996. Testing ecological models: the meaning of validation. Ecol. Model. 90, 229–244.
Sandgren, C.D., 1991. Growth and Reproductive Strategies of Freshwater Phytoplankton. Cambridge University Press.
Snodgrass, W.J., Ng, P.S., 1985. Biochemical models for the hypolimnetic oxygen depletion in lakes impacted by wastewater discharges: 2. Phytoplankton biomass model. Arch. Hydrobiol. Supp. 72 (2), 220–236.
Sommer, U., 1989. Phytoplankton ecology. Succession in Plankton Communities. Springer-Verlag.
Soranno, P.A., 1997. Factors affecting the timing of surface scums and epilimnetic blooms of blue-green algae in a eutrophic lake. Can. J. Fish. Aquat. Sci. 54 (9), 1965–1975.
Sterner, R.W., Elser, J.J., Hessen, D.O., 1992. Stoichiometric relationships among producers, consumers, and nutrient cycling in pelagic ecosystems. Biogeochemistry 17, 49–67.
Tian, R.C., Vezina, A.F., Starr, M., Saucier, F., 2001. Seasonal dynamics of coastal ecosystems and export production at high latitudes: a modeling study. Limnol. Oceanogr. 46 (8), 1845–1859.
Van Arkel, G.J. 1993. Long-term sediment modeling in Hamilton Harbour, M.Sc. Thesis, Civil Engineering, McMaster University, Ontario, Canada.
Watson, S.B., Ridal, J., Boyer, G.L., 2008. Taste and odour and cyanobacterial toxins: impairment, prediction, and management in the Great Lakes. Can. J. Fish. Aquat. Sci. 65 (8), 1779–1796.
Wetzel, R.G., 2001. Limnology: Lake and River Ecosystems, 3rd ed. Academic Press, New York, USA.
Wroblewski, J.S., 1977. Model of phytoplankton plume formation during variable Oregon upwelling. J. Mar. Res. 35 (2), 357–394.
Zhang, W., Arhonditsis, G.B., 2008. Predicting the frequency of water quality standard violations using Bayesian calibration of eutrophication models. J. Great Lakes Res. 34, 698–720.